NASA Technical Paper 3489

August 1994

Evaluation of COSTAR Mass Handling Characteristics in an Environment – A Simulation of the Hubble Space Telescope Service Mission

Sudhakar L. Rajulu,
Glenn K. Klute, and
Lauren Fletcher

NASA Technical Paper 3489

August 1994

Evaluation of COSTAR Mass Handling Characteristics in an Environment – A Simulation of the Hubble Space Telescope Service Mission

Sudhakar L. Rajulu, Ph.D.
Lockheed Engineering & Sciences Company
Houston, Texas

Glenn K. Klute, M.D., and
Lauren Fletcher
Flight Crew Support Division
Lyndon B. Johnson Space Center
Houston, Texas

National Aeronautics and
Space Administration

This publication is available from the NASA Center for AeroSpace Information, 800 Elkridge Landing Road, Linthicum Heights, MD 21090-2934 (301) 621-0390.

Contents

Figures

Tables

Acronyms

ANOVA	univariate analysis of variance
COSTAR	Corrective Optics Space Telescope Axial Replacement
DSO	detailed supplementary objective
EVA	extravehicular activity
HST	Hubble Space Telescope
JE	Johnson Engineering
JSC	Johnson Space Center
LESC	Lockheed Engineering and Sciences Co.
MANOVA	multivariate analysis of variance
PABF	precision air bearing facility
PFR	portable foot restraint
ORU	orbital replacement unit
RMS	remote manipulator system
WF/PC	wide field planetary camera

Acknowledgments

We acknowledge Richard Fullerton of the Johnson Space Center (JSC) Mission Operations Directorate for bringing this project to our attention and arranging the test subjects and crew for this study. He was also responsible for coordinating our efforts in setting up the Precision Air Bearing Facility (PABF). Our heartfelt thanks go to Bill Lee (Johnson Engineering (JE)) and John Harvey (JE) in Building 9 at JSC. They were very helpful in building the sled and the COSTAR [Corrective Optics Space Telescope Axial Replacement] mockup and helped us meet our deadline. They even modified the mockups and setup so that the STS-61 crew could get additional training on the PABF. Thanks go to Steve Pybus (JE) for doing the structural analysis of the mockups and for making sure the mass characteristics of the mockups matched those of the actual orbital replacement units. We also thank Tom Smith (NASA) in Building 9, JSC, for providing facility support throughout this project. We especially thank Robert Wilmington (Lockheed Engineering and Sciences Co. (LESC)) for his active role during this project; Ralph Wemhoff (LESC) for his technical support; Dishayne Garcia (NASA Co-Op) for giving us a hand during the project; and Lara Stoycos (LESC) for editing this report.

Executive Summary

The STS-61 mission, which took place in December 1993, was solely aimed at servicing the Hubble Space Telescope (HST). Successful completion of this mission was critical to NASA, since it was necessary to rectify a flaw in the HST mirror. In addition, NASA had never scheduled a mission that required such a quantity of complex extravehicular activity (EVA).

To meet the challenge of this mission, STS-61 crew members were trained extensively in the Weightless Environment Test Facility (WETF) at the Johnson Space Center (JSC) and in the Neutral Buoyancy Simulator at the Marshall Space Flight Center. It was suspected, however, that neutral buoyancy training might induce negative training because of the viscous damping effect in water. Mockups built for this training also did not have the mass properties of the actual orbital replacement units (ORUs). It was thus felt that the STS-61 crew should be further trained on mockups with similar mass characteristics.

Unfortunately, mockups with similar mass properties cannot be made easily for a water environment. Thus, owing to the suspected negative training in the WETF and the need to train with ORUs of actual mass properties, it was decided to conduct additional training at the Precision Air Bearing Facility (PABF). The Flight Directorate wanted to know whether the crew would encounter any problems if the remote manipulator system (RMS) suddenly stopped or started. Hence, a comprehensive study was designed to address these issues. The study was quantitative, and instrumentation was set up to measure and quantify the forces and moments experienced during ORU mass handling and RMS run conditions.

Four suited test subjects were involved in the study. Tests were conducted on the PABF in Building 9 at JSC. Mockups were built to match the mass characteristics of the actual ORUs, and both mockups and subjects were supported by air sleds that allowed nearly friction's travel across the floor. A load relief provided support to the subjects. Fixtures were made with rope and bungee to simulate a sudden RMS start or stop condition.

Controlled tasks were first performed in X and Y translations and in yaw, pitch, and roll rotations to evaluate quantitatively the forces and moments that could be exerted by the subjects during ORU mass handling. Forces and moments generated during these controlled tasks were then compared to the forces and moments generated during sudden RMS run conditions.

Data collected from the study were statistically analyzed—first to compare the effort required to perform any controlled translation and rotation, and then to determine the maximum effort exerted by subjects during different phases of RMS conditions. The overall results from this study showed that the

forward force component (F_x) was two times greater during a stopping condition than during a controlled ORU handling task. With the exception of this force component, all other force and moment components were similar to those that would be obtained during a controlled task. Subsequent biomechanical analysis showed that the strength requirements of such a condition were well within the capacities of the STS-61 crew members.

1.0 Introduction

The STS-61 mission, which took place in December 1993, was solely aimed at servicing the Hubble Space Telescope (HST) launched in 1991. While HST had been providing valuable information to NASA scientists and astronomers worldwide, modifications were necessary to correct the degraded performance of several components including a flaw in the HST mirrors. Hence, NASA scheduled the STS-61 mission to service the HST by replacing the Corrective Optics Space Telescope Axial Replacement (COSTAR) and the wide field planetary camera (WF/PC). In addition to servicing these orbital replacement units (ORUs), STS-61 crew members replaced the HST solar arrays and performed several other maintenance operations. Appendix A includes photographs of the HST, COSTAR, WF/PC, and solar arrays.

Successful completion of this mission was extremely important to NASA for several reasons. First and foremost, it was critical that NASA rectify the flaw in the HST mirror. Without a correction to this optical flaw, usefulness of the HST in the visible light spectrum would have continued to be less than optimal to support data collection by NASA and the scientific community. Second, although NASA had considerable experience in on-orbit extravehicular activities (EVAs), it had never performed such a quantity of complex EVAs as was scheduled for this mission. Servicing the HST required 5 consecutive days of EVA and placed high demands on the crew members and the ground team. Third, this EVA mission was perceived to be an indication of NASA preparedness to build and maintain a space station. Positive results were needed to demonstrate EVA capability for such important missions. Quality training, therefore, had to be provided so that there were no significant surprises during the tasks (Table 1) of this mission.

Table 1: Tasks performed by the STS-61 crew

1. Retrieve HST and bring it to the Shuttle payload bay using the remote manipulator system (RMS).
2. Remove the existing ORUs and solar panels from the HST and stow them temporarily.
3. Pick up the new ORUs and the solar arrays from the storage and install them in/on the HST.
4. Store the old ORUs in the payload bay.
5. Verify the performance of the new ORUs and deploy the HST.

To perform all these tasks, the crew had to depend extensively on the RMS and to manually handle many small components as well as fairly large masses. The COSTAR and the WF/PC weighed approximately 2675.5 N (600 lb), and each solar array weighed approximately 1471.5 N (330 lb).

To successfully meet the demands of this mission, the STS-61 crew trained at many facilities, including the Weightless Environment Training Facility (WETF) at the Johnson Space Center (JSC) and the Neutral Buoyancy Simulator at the Marshall Space Flight Center. These facilities are large swimming pools which offer a neutral buoyancy environment that allows crew members to work within a free-floating environment continuously. Much of the EVA training is done in these facilities by crew members who are wearing pressurized suits. During training, crew members perform EVA tasks to gain a sense of doing those tasks in a zero-g environment and, for this mission, an understanding of end-to-end HST maintenance procedures and hardware manipulation.

Though the neutral buoyancy environment provides valuable benefits in terms of training the crew in a simulated zero-g environment, it has an undesirable negative effect because of the viscosity of the water. In true zero g, there is no appreciable friction. However, because of the viscosity of water, non-flight drag forces are inevitable during neutral buoyancy simulation, unless the tasks are performed at a slow velocity. In general, the crew performed the underwater training at a slow pace; hence, the drag forces were relatively low. Unfortunately, in true zero g, the water damping effects that make the crew member's body and other objects inherently stable are not present. Subtle disturbances from crew handling forces are no problem during training, but they can be a major problem on orbit. Water drag also makes large mass handling impractical underwater, since the manual control forces are artificially excessive. Thus, crew members on a few of the previous EVA-related missions were surprised by the absence of non-flight forces and found their tasks more difficult to perform on orbit than during ground training. Hence, there was a concern that underwater facilities might induce negative training because of the viscous damping of water.

Owing to this concern over negative training and the significance of the STS-61 mission, NASA was interested in providing an additional method of training for the STS-61 EVA servicing tasks. As in the past, the Precision Air Bearing Facility (PABF) was considered the best alternative to supplement the underwater training. The purpose of the PABF exercise was to simulate the loads imparted to and by crew members while handling ORUs without the extraneous resistance induced by water viscosity.

The PABF is located in Building 9 at JSC. It is one of several zero-g simulation facilities at the Center. The PABF is made of stainless steel floor plates that cover an area 7.31 m x 9.75 m (24 ft x 32 ft). The floor is machined smooth to within 0.0254 mm (0.002 in.) and is level to within 0.0762 mm (0.003 in.). With these tight tolerances and this smooth finish, air bearing pads are used

to support objects and personnel on a nearly friction-free environment. Unlike the underwater training environment, the PABF provides an environment in which a crew member can experience the effect of performing a task that is almost frictionless and with more or less similar mass characteristics. However, the effect of Earth gravity is still present in directions other than those parallel to the floor plane. It should be borne in mind that training on the PABF alone is not sufficient to fully acclimate a crew to the zero-g environment; however, it does eliminate the water drag forces present in the neutral buoyancy environment and realistically prepares crew members for the fine fingertip manual control of masses actually required on orbit.

2.0 Objectives

The purpose of this study was to validate the training techniques planned for STS-61 crew members in a simulated zero-g environment. More specifically, it was intended to simulate and monitor the reaction of test subjects who were maneuvering the ORUs and during a sudden RMS run start/stop condition.

The RMS run condition refers to a situation in which a crew member who is positioned in the portable foot restraint (PFR) at the end of the robotic arm maneuvers the ORU by holding onto the ORU handrails. Though flight conditions are usually more benign, the RMS run start/stop condition refers to a worst-case situation in which the RMS comes to a sudden stop or starts suddenly without issuing a prior warning. One of the concerns raised by NASA was whether a crew member would be able to respond to the unlikely situation of the RMS coming to a sudden stop or start. Since this scenario was not included in the WETF training protocol, it was included in the PABF training protocol. It was thus hoped that this study would provide information concerning whether the crew, while moving the ORUs during the RMS operations, could react to, and counteract comfortably, those forces imparted by the simple motions of mass and inertia.

3.0 Methodology

3.1 Subjects

Four subjects participated in our study. All subjects were suit qualified and had passed the Air Force Class III physical examination. Their age ranged from 20 to 35 years, with a mean of 27 years. Their stature ranged from 160 to 180 cm. All subjects had previous experience in a pressurized Space Shuttle suit.

3.2 Apparatus

Tests were conducted on the PABF. Mockups were built to simulate the mass characteristics of the COSTAR and the WF/PC. The mockup dimensions and mass properties matched those of the actual ORUs. After the mockups were built, their mass characteristics were verified. Appendix B contains the calculations and details of this verification process. The COSTAR was built with aluminum uni-strut frames; the WF/PC was built primarily of wood. Both mockups had 5 degrees-of-freedom[1] (X, Y, yaw, roll, and pitch). Neither had the capability to move in the Z direction (up and down) in real time, except between tests to accommodate subjects of different heights and to achieve a desired body position. X and Y translations were achieved by moving the mockup on the floor along its axes. Yaw, pitch, and roll motions were obtained by placing a ball-and-socket joint at the pivot. This joint was an air-bearing device for the WF/PC and a mechanical unit for the COSTAR. Yaw motion refers to rotational motion that occurs about the vertical axis. Pitch motion refers to rotation that occurs at the pivot about an axis that runs parallel to the front and back panels of the mockup. Roll motion refers to rotation that occurs at the pivot about an axis that runs parallel to the side panels of the mockup (see Figure 1 for coordinate definition).

Force plates were attached to both the COSTAR and the WF/PC mockups to measure forces and moments exerted by crew members at the ORU handrails. Accelerometers were used to determine the amount of pitch and roll and the acceleration in the X and Y axes during motion. Signals from the force plates and the accelerometers were fed through amplifiers into a data acquisition system. The data collection rate was 250 Hz, and the data collection period was 20 sec. Data were taken only during COSTAR mockup trials.

---

[1]In this paper, axes are represented with capital letters (X, Y, and Z) which refer to the floor coordinate system. That is, the X and Y axes are on the floor surface and the Z axis is the vertical axis. Forces and moments in each of these axes are represented with lowercase letters. In this study, the force plate was attached to a vertical plane rather than to the floor. Hence, a push or pull would result in a z force according to the convention used by the force plate. However, for easy understanding, forces and moments are represented with respect to the floor coordinate system.

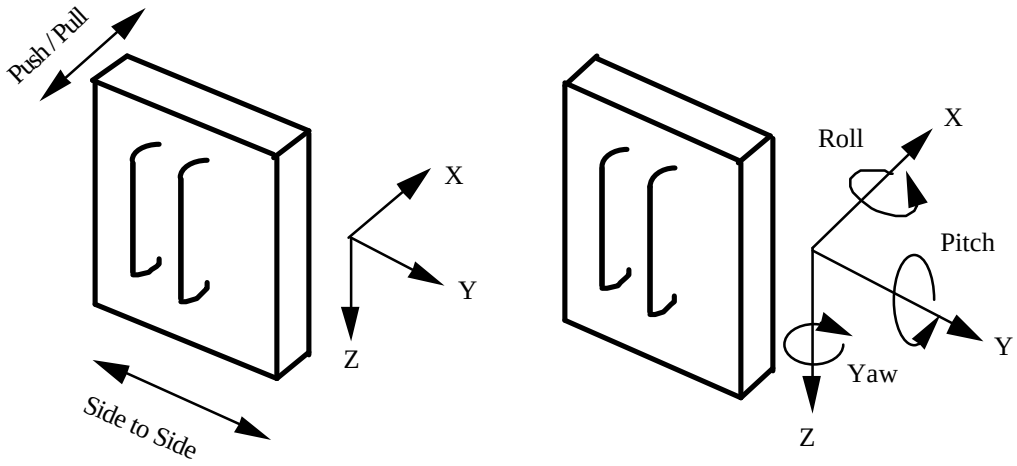

Figure 1. Representation of forces and moments

Data were taken only during COSTAR mockup trials, primarily because of the non-availability of instrumentation to measure forces around the WF / PC handles and a limited quantity of accelerometers. Both ORUs were later used to train the crew members, however. Figures 2 and 3 show the front and back views of the COSTAR mockup (the front view shows the handrails; the back view shows the weights for correct mass properties).

Three video cameras were used to obtain video data for motion analysis. One camera was mounted from the ceiling, directly over the center of the PABF. This camera provided a top view of the ORU. Two other cameras that were positioned at a 45° angle from the center line of the floor were used to conduct three-dimensional motion analysis.

3.3 Experimental Design

The main objective of this study was to determine the forces and moments applied and encountered by test subjects during the RMS run start / stop condition. More specifically, this study was designed to determine whether a crew member would be able to withstand the impact of a sudden RMS run start / stop and continue to hold onto the ORUs without exerting or experiencing uncontrollably large forces or moments.

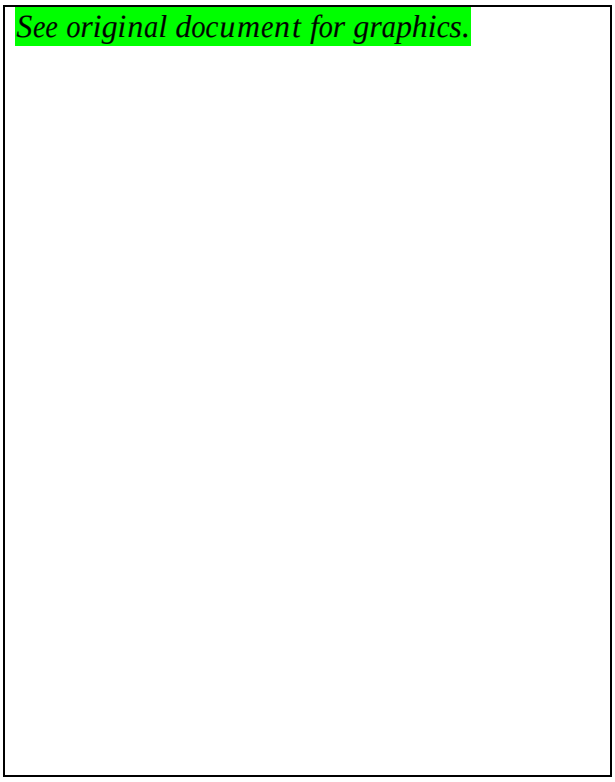

Figure 2. Front view of the COSTAR mockup

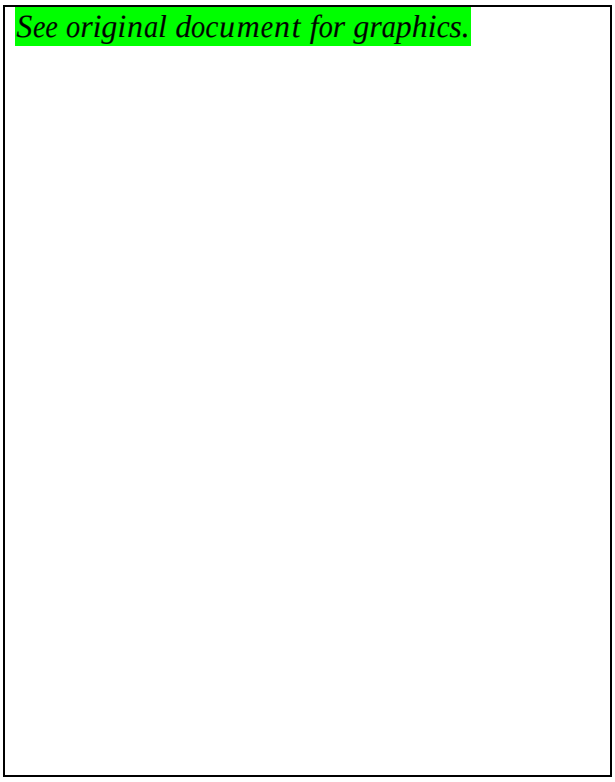

Figure 3. Back view of the COSTAR mockup

First, to determine how large the forces and moments are during RMS operations, controlled mass handling situations were included in the study. These controlled motions were:

- push / pull translation,
- side to side translation,
- yaw rotation,
- pitch rotation, and
- roll rotation.

Second, to see the effect of velocity on these forces and moments, RMS conditions were tested at two velocities; namely, 1 fps and 2 fps. The nominal course rate set for the STS-61 mission was 0.7 fps. Velocity values for this study were chosen primarily to represent this nominal course rate as well as to determine the handling margin. The handling margin provided a scenario in which the velocity was twice the recommended rate.

Third, to assess the impact on a temporal basis, the RMS run start / stop condition was divided into three phases. These phases were: start, stop, and stabilize.

Thus, the independent variables in this study were push / pull translation, side to side translation, yaw, pitch, and roll; RMS run speed—slow and fast; and RMS run stages—start, stop, and stabilize. The dependent variables were x, y, and z forces; and x, y, and z moments.

Two additional studies were performed in conjunction with this study. One of these involved calibrating the system to obtain data for use in a mathematical modeling of the trajectory of the ORUs. The purpose of this model was to predetermine the path of motion of the ORU given an initial force and to compare that path to the actual path or trajectory experienced during the STS-61 mission. Results of this modeling effort can be found in the report by Cuthbert et al. (1993). The second study quantified the ORU movement errors caused by factors such as drag of the air-pressure hoses which provided air to the pads on the air bearing sleds. Results from this study can be found in the report by Stoycos et al. (1993). In this report, only the second phase of the study will be discussed.

3.4 Experimental Procedure

The experiment took place over 4 days. One subject performed the experiment each day. At the start of the experiment the subject, with the help of suit technicians, donned the suit and adjustments were made to the suit to make it comfortable. An overhead crane provided a load relief system from above. This load relief allowed reasonable mobility and prevented the subject from tipping over. Prior to performing the task, each subject was briefed on the

procedure and was given time to practice manipulating the mockup ORUs. Administration of the task conditions remained the same for all subjects, and three trials were taken for each of these task conditions. The subject performed the push/pull translation (Figure 4) first, then the side to side translation (Figure 5), and finally the yaw translation. All three tasks took place with the subject standing firmly on the PABF. The COSTAR was brought down as low as possible and was fastened so that neither pitch nor roll was possible. For these tasks, the air pads were turned on to allow free movement of the ORU across the floor. The subject then performed the pitch and roll rotations (Figure 6). For these two tasks, the air pads were turned off to eliminate any translation movement, and the ORU was raised to a height that allowed sufficient pitch and roll ranges of motion. The subject was instructed to perform these tasks slowly to isolate the pitch and roll motions from one another.

After completing these five translation and rotation tasks, the subject performed the RMS run start/stop task (Figure 7). In this, the subject was positioned standing in the PFR which was mounted on one of the sleds. The purpose of this task was to simulate the sudden starting or stopping motion of the RMS. However, RMS flexibility and its effects on mass handling control were not simulated in any portion of these tasks. The RMS rate was simulated using a bungee cord and a rope. The bungee cord was looped around the front end of the sled and around two stationary posts in front of the sled. The bungee cord provided a damping effect (constant acceleration/ deceleration). A rope connected the back of the sled to another post at the back of the sled, permitting approximately 10 ft of travel before coming to a stop. The subject's sled was initially positioned close to the back post, thus putting a slack in the rope and stretching the bungee cord. The COSTAR was brought close to the subject's sled, and the air pads for both the COSTAR and the subject were turned off. The height of the COSTAR was adjusted so that the subject could hold the handrails with elbows at right angles.

Once the subject and the sleds were properly positioned, data collection was initiated and air pads for the COSTAR were turned on. The subject then grabbed the handrails and, within a few seconds, the air pads for the sled were turned on. Since the bungee had been stretched prior to the task, when the air was turned on the sled traveled forward. The travel of the sled was manually controlled by a person holding the sled and providing resistance so that the speed was either (approximately) 1 fps or 2 fps. As the sled moved forward, the subject held onto the handrails. As soon as the rope at the back of the sled became taut, the sled came to a sudden stop. The subject was instructed to hold onto the handrails and arrest the motion of the COSTAR. The subject then stabilized the COSTAR and, after a few seconds, released the handrails. These RMS run start/stop trials were performed at two different velocities: 1 fps and 2 fps.

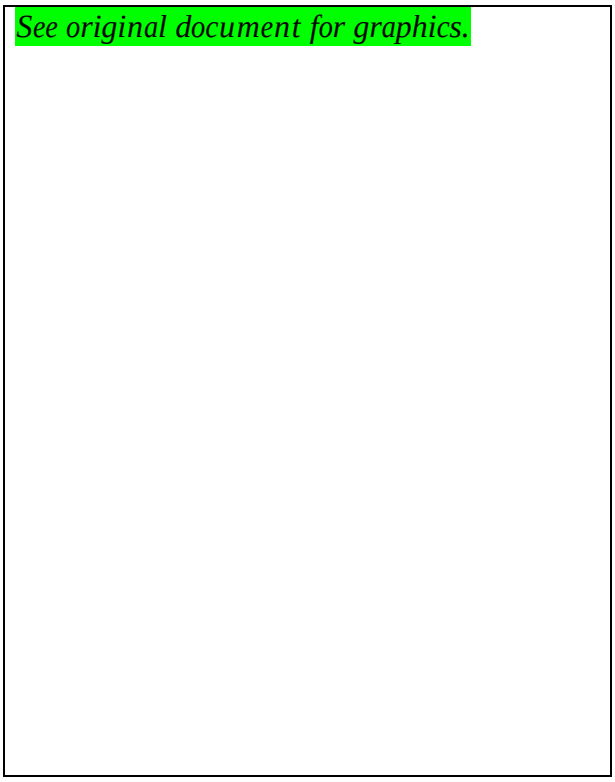

Figure 4. Subject performing push/pull translation task

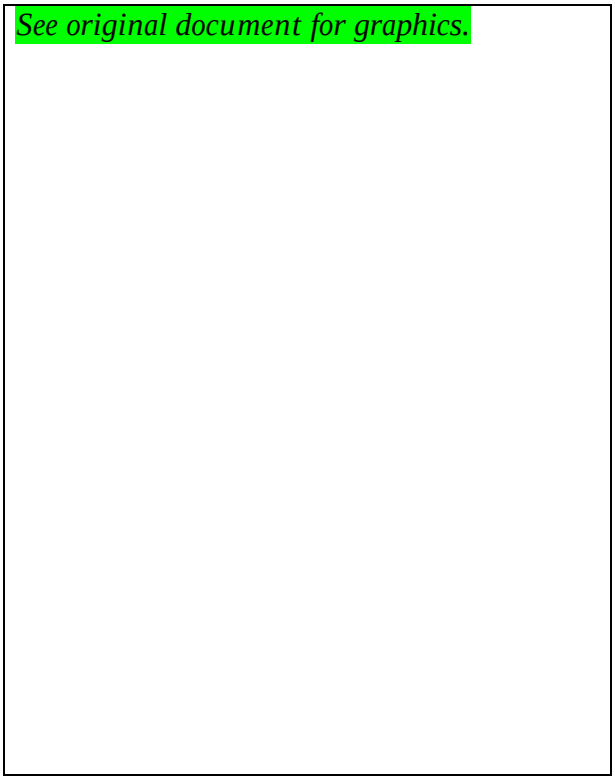

Figure 5. Subject performing side to side translation task

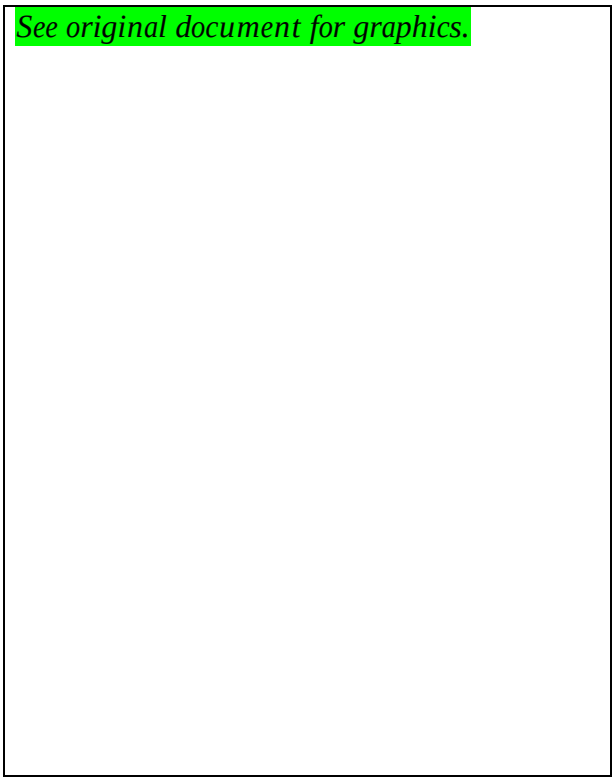

Figure 6. Subject performing pitch rotation task

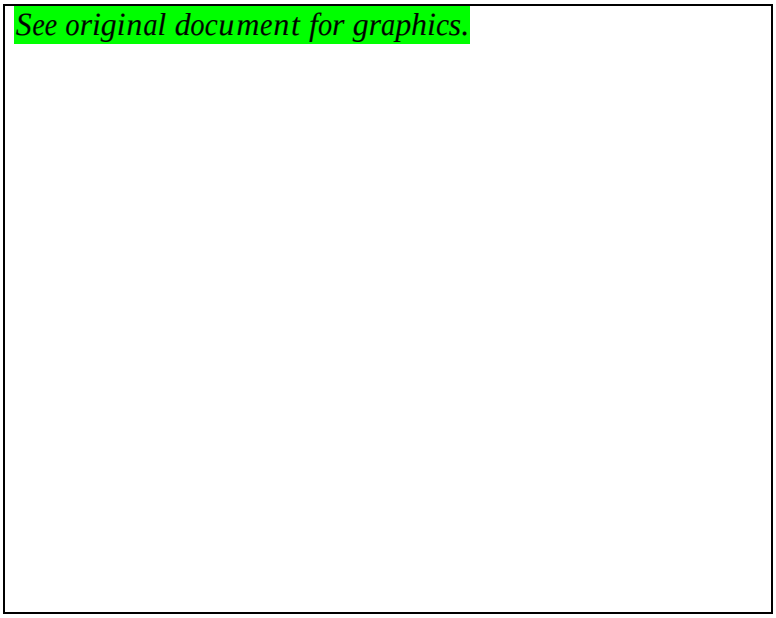

Figure 7. Subject performing RMS run start/stop task

3.5 Data Treatment

For this study, only force plate data were analyzed. Data from the accelerometers were used solely to calibrate and model the motion characteristics. More details on the accelerometer data can be found in Cuthbert (1993). For the five translation and rotation tasks, the force plate data were treated as follows.

For each of these tasks, the subject performed either push / pull, side to side translation, or yaw, pitch, or roll rotations. Each task resulted in a greater force or moment in one primary axis or plane (X, Y, or Z). For the RMS run start / stop tasks, the data were split into three phases. These phases were starting, stopping, and stabilizing. Table 2 shows the primary force / primary moment axis or plane for all these tasks.

Table 2: Primary force and moment axes/planes for translation and rotation tasks

Task	Primary Force	Primary Moment
Push / pull	X	
Right / left	Y	
Yaw		Z
Pitch		Y
Roll		X
RMS	X	X, Z

First, the peak value and temporal location of either the primary force or moment were determined for each task and for each direction of motion. Once the temporal location was known, the other components of force and moment were determined. The forces and moments were gathered for each task and were entered into a database and transferred to the mainframe VAX computer for statistical analyses.

3.6 Statistical Analyses

Owing to the fact that the translation and rotation data and RMS data relate to different aspects of COSTAR mass handling, two separate analyses were performed. The first analysis tested the variation among different means of translating and rotating COSTAR (i.e., X, Y, yaw, pitch, and roll), and the second analysis compared the aspects of RMS starting, stopping, and stabilizing of the COSTAR at two different velocities.

Multivariate analyses of variance (MANOVAs) were performed, followed by univariate analysis of variance (ANOVA), for both sets of data. For the translation data set, the means of translation served as the independent variable. Because of our small sample size, the interaction term (subject*means of translation) was used as the error term. For the RMS run start/stop data set, phase of motion and velocity served as independent variables.

4.0 Results

4.1 Translation and Rotation Tasks

The MANOVA on the translation and rotation data showed that dependent measures (i.e., forces and moments) as a whole were affected significantly by the means of translation (Wilk's test: $F(24,26) = 4.79$; $p = 0.001$). The ANOVA showed that the three force components and the three moment components were (individually) affected significantly by a change in means of translation ($p < 0.0001$). Subsequent multiple comparison tests revealed the following results (Tables 3 to 8).

The F_x component (Table 3) was significantly higher during push / pull, pitch, and roll motions than during yaw and side to side motions. F_x was greatest for push / pull translation (46.8 N; 10.5 lb) and least for side to side translation (9.3 N; 2.1 lb). Statistically, there were no significant differences between push / pull, pitch, and roll motions or between side to side and yaw motions. During push / pull, pitch, and roll motions, however, the force in the x direction was twice as great as during side to side and yaw motions.

Table 3: Mean F_x as a function of task condition

Condition	Mean value (N)	Grouping[2]
Push / pull	46.8	A
Yaw	15.1	B
Side to side	9.3	B
Pitch	33.1	A
Roll	32.2	A

The mean force component F_y (Table 4) was significantly less during push / pull (7.2 N; 1.6 lb) than during the other means of translation. During pitch, the mean F_y was also significantly less than during side to side translation, yaw, and roll (15.8 N; 3.54 lb). There were no differences in F_y among the yaw, side to side translation, and roll.

[2]Same letter grouping denotes there is no statistical significance within the same grouping.

Table 4: Mean F_y as a function of task condition

Condition	Mean value (N)	Grouping[3]
Push / pull	7.2	C
Yaw	36.9	A
Side to side	34.2	A Pitch
15.8	B	
Roll	33.9	A

The mean force component F_z (Table 5) was significantly greater during push / pull translation (54.1 N; 12.1 lb) than during all other means of translation. There were no significant differences in F_z between side to side and yaw motions (31.6 N; 7.1 lb vs. 36.8 N; 8.3 lb). However, during side to side translation, F_z was significantly greater than during pitch and roll motions (22.5 N; 5.01 lb and 20.0 N; 4.9 lb).

Table 5: Mean F_z as a function of task condition

Condition	Mean value (N)	Grouping[3]
Push / pull	54.1	A
Yaw	36.8	B
Side to side	31.6	B C
Pitch	22.5	D C
Roll	20.0	D

The moment M_x (Table 6) was significantly higher for roll (13.8 Nm; 19.16 ft·lb) than for pitch rotation (8.7 Nm; 6.4 ft·lb), which in turn was higher than the rest of the translations. The moment component M_y (Table 7) was significantly higher during pitch rotation than during the other four translations (11.9 Nm; 8.76 ft·lb). On the other hand, M_z (Table 7) was significantly higher for yaw translation than during push / pull and side to side translations (15.4 Nm; 11.3 ft·lb vs. 8.7 Nm; 6.4 ft·lb, 8.2 Nm; 6.03 ft·lb). M_z was significantly lower for the remaining translations; namely, the roll and pitch rotations (4.8 Nm; 3.53 ft·lb and 3.9 Nm; 2.9 ft·lb). The lowest moment was produced around the X axis (2.6 Nm; 1.91 ft·lb).

[3]Same letter grouping denotes there is no statistical significance within the same grouping.

Table 6: Mean M_x as a function of task condition

Condition	Mean value (Nm)	Grouping[4]
Push / pull	2.6	C
Yaw	3.9	C
Side to side	4.7	C
Pitch	8.7	B
Roll	13.8	A

Table 7: Mean M_y as a function of task condition

Condition	Mean value (Nm)	Grouping[4]
Push / pull	7.7	B
Yaw	7.1	B
Side to side	6.4	B
Pitch	11.9	A
Roll	7.0	B

Table 8: Mean M_z as a function of task condition

Condition	Mean value (Nm)	Grouping[4]
Push / pull	8.7	B
Yaw	15.4	A
Side to side	8.2	B C
Pitch	3.9	D
Roll	4.8	D C

[4]Same letter grouping denotes there is no statistical significance within the same grouping.

Figures 8(a) and (b) provide graphical representations of force and moment components during the translation and rotation tasks, respectively.

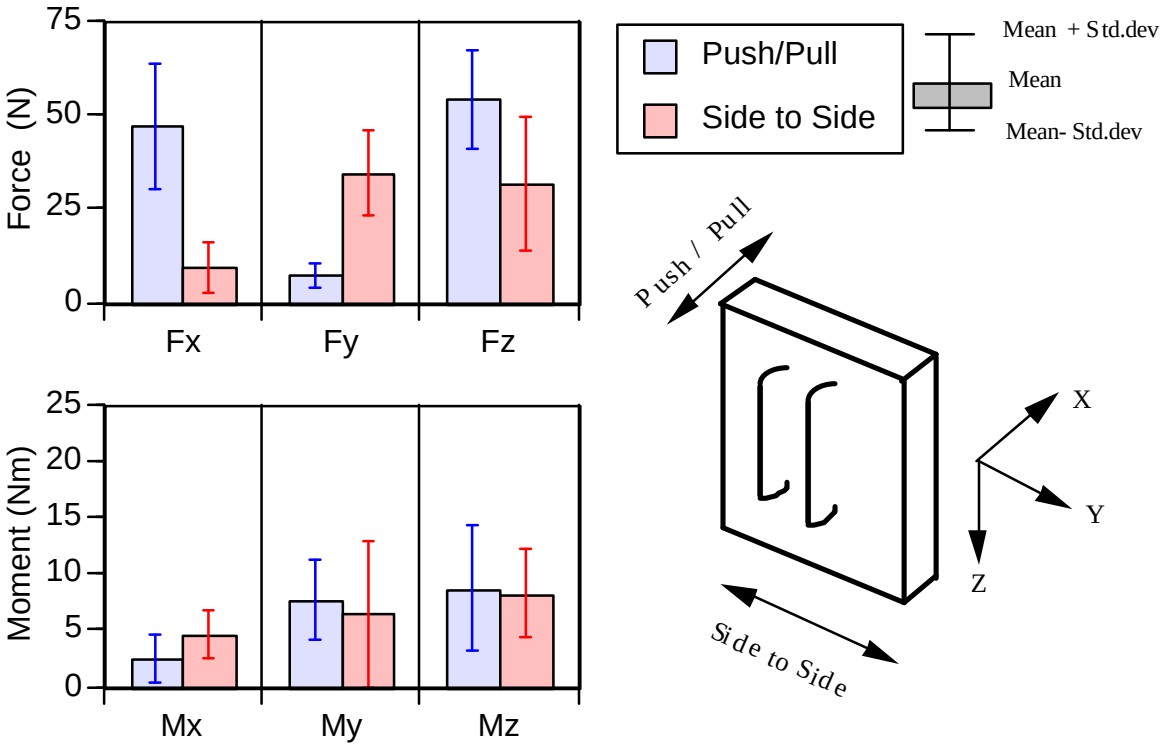

Figure 8(a). Mean forces and moments during translation tasks

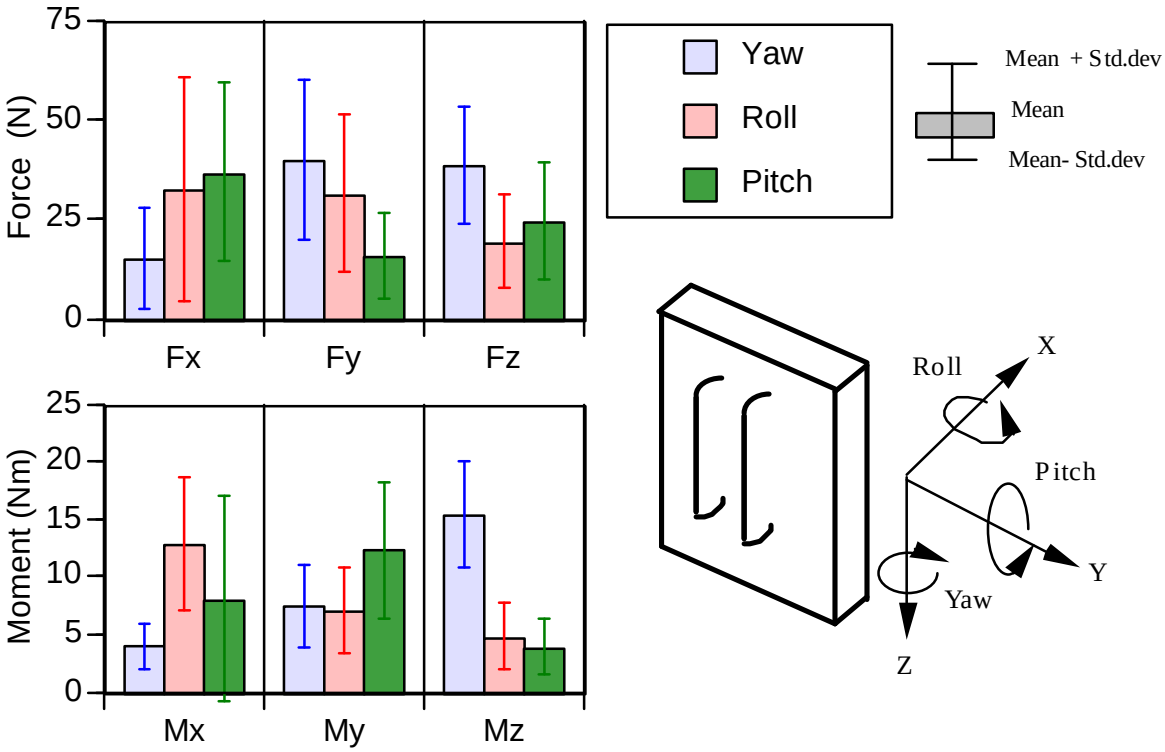

Figure 8(b). Mean forces and moments during rotation tasks

The previously described analyses were based on variations in the absolute forces and moments exerted by test subjects. The following section decomposes these forces and moments by direction and, thus, further details how the subjects performed these tasks. Figure 9 shows the average forces and moments exerted by subjects during the push / pull task. As can be seen in these figures, equal amounts of force in the X axis were exerted during pushing and pulling. It is also apparent that the subjects exerted a greater upward force than a downward force (F_z). A significant upward force during pushing and pulling could be attributed to the subjects trying to keep the ORU straight. Moments were rather equal during pushing and pulling. It should also be noted that test subjects tended to pitch forward (M_y, Figure 9) and to roll to the right rather than to the left (M_x, Figure 9).

Figure 10 shows the average forces and moments exerted by subjects during the side to side translation task. As can be seen in the figure, an equal amount of force (F_y) was exerted in both the right and left directions. Again, subjects tended to apply more force (F_z) in the upward direction. Figure 11 shows the average forces and moments exerted by subjects during yaw motion. With the exception of M_x and M_z, forces and moments were even during left and right yaw. Figure 12 shows the average forces and moments exerted by subjects during roll motion. In general, test subjects tended to exert more moment while rolling to the right side than while rolling to the left side (M_x, Figure 12). Figure 13 shows the average forces and moments exerted by subjects during pitch motion.

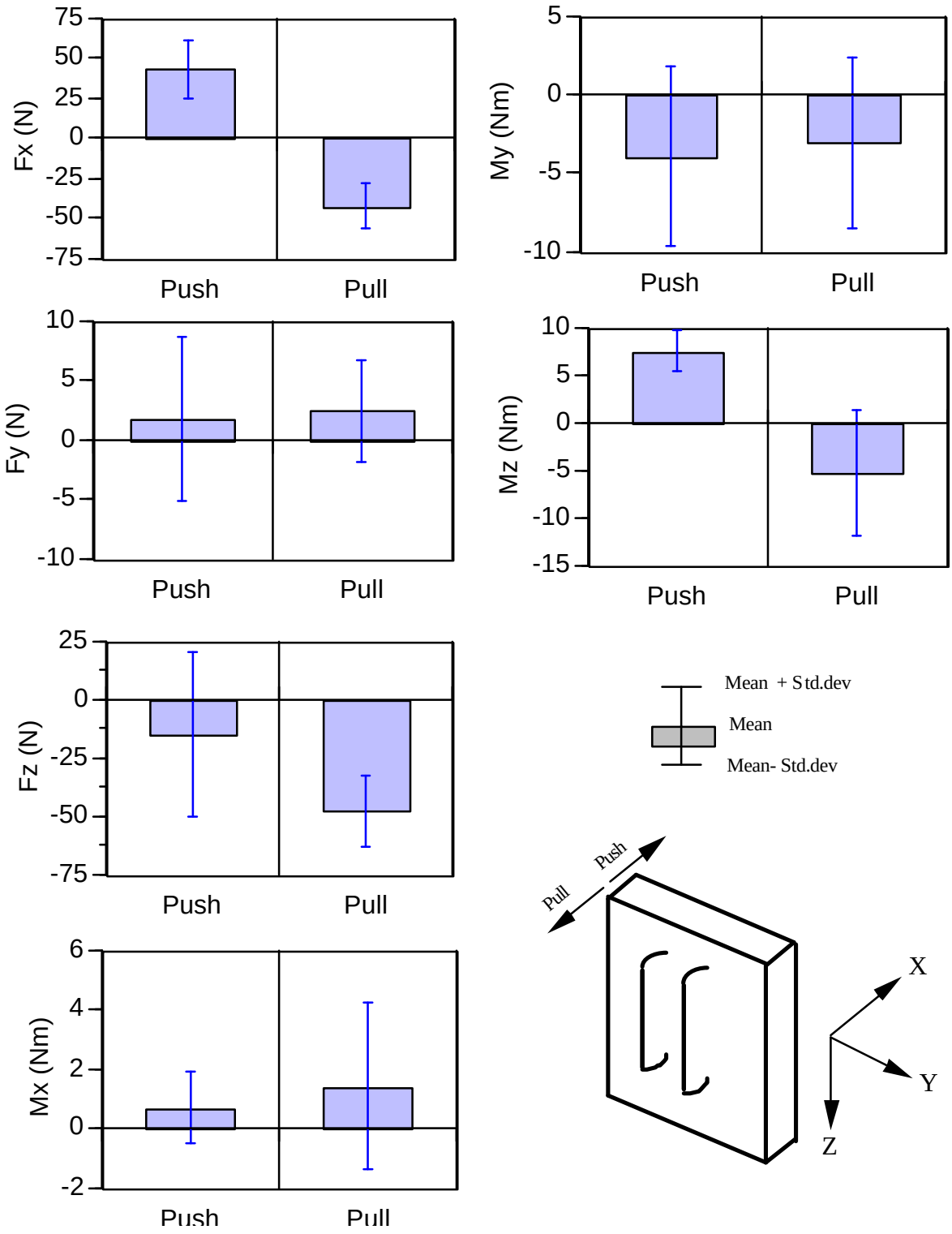

Figure 9. Forces and moments during push/pull tasks

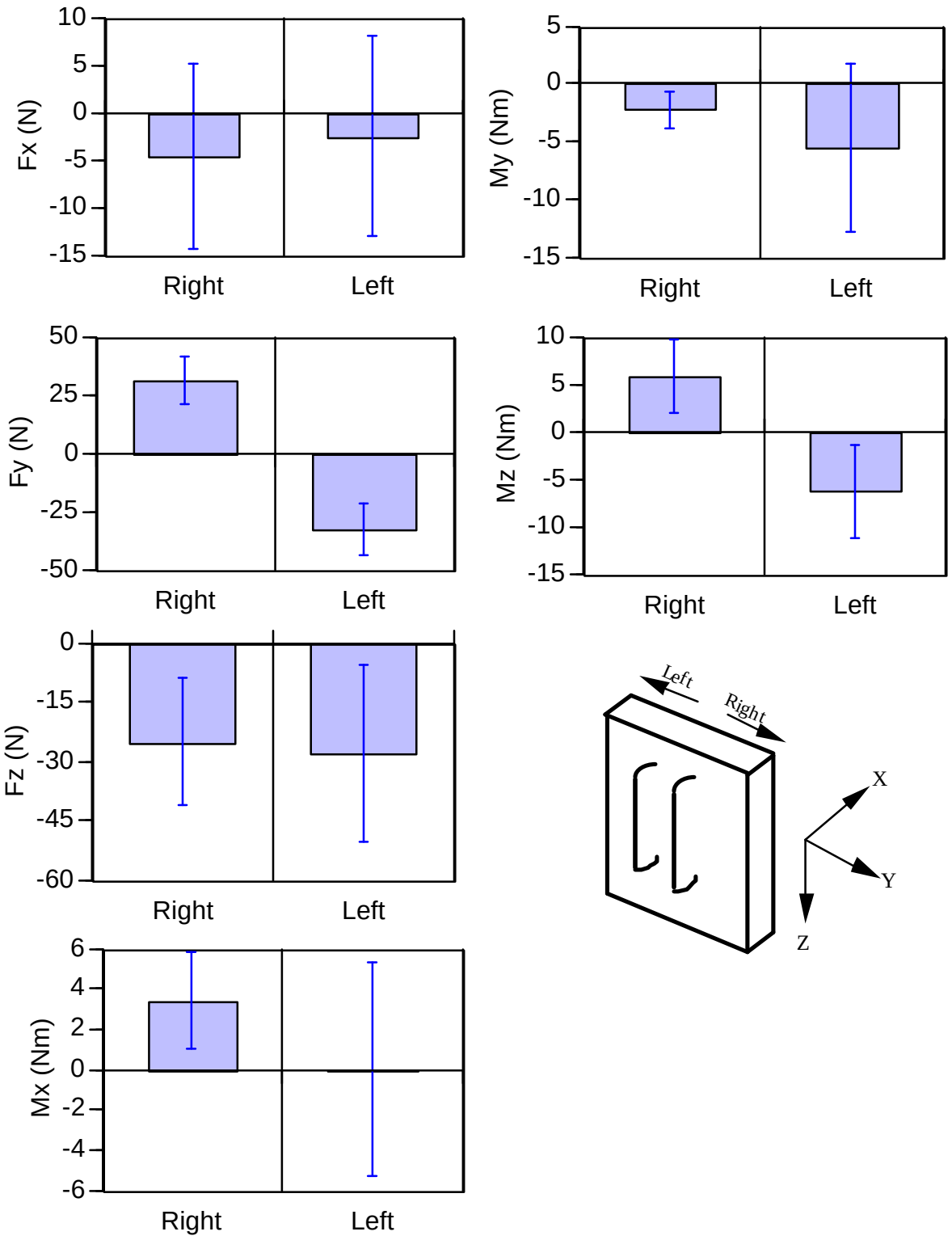

Figure 10. Forces and moments during side to side translation tasks

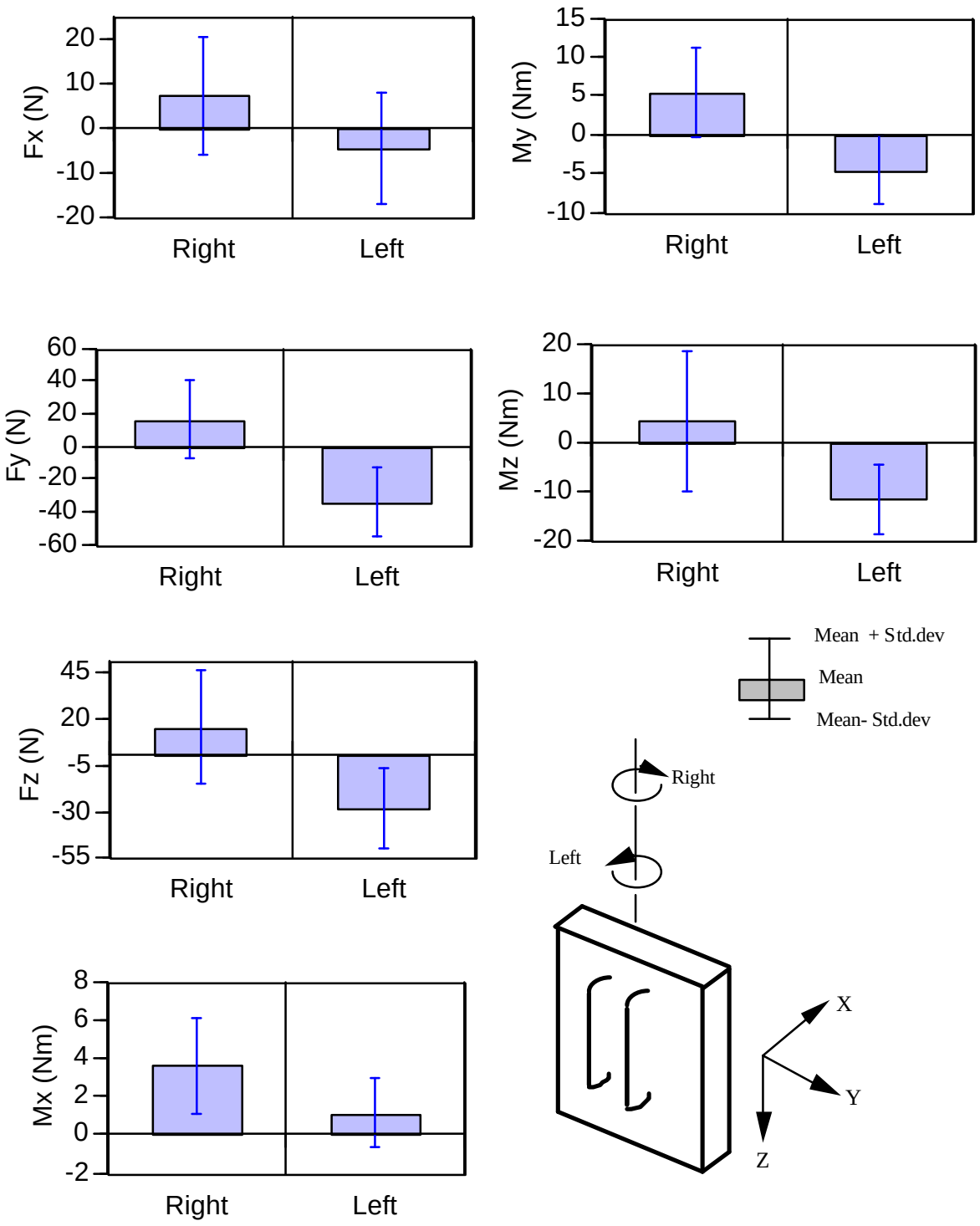

Figure 11. Forces and moments during yaw rotation tasks

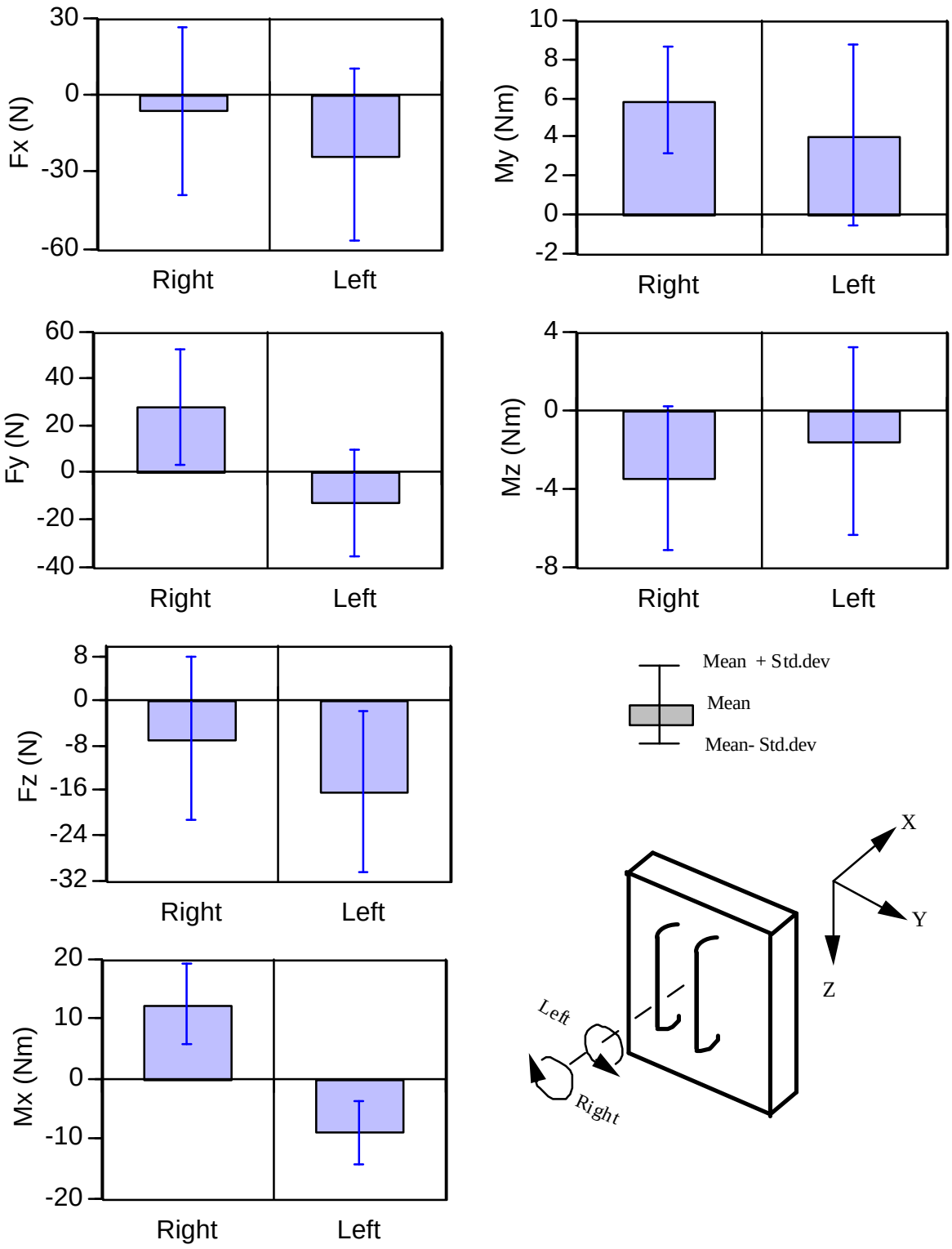

Figure 12. Forces and moments during roll rotation tasks

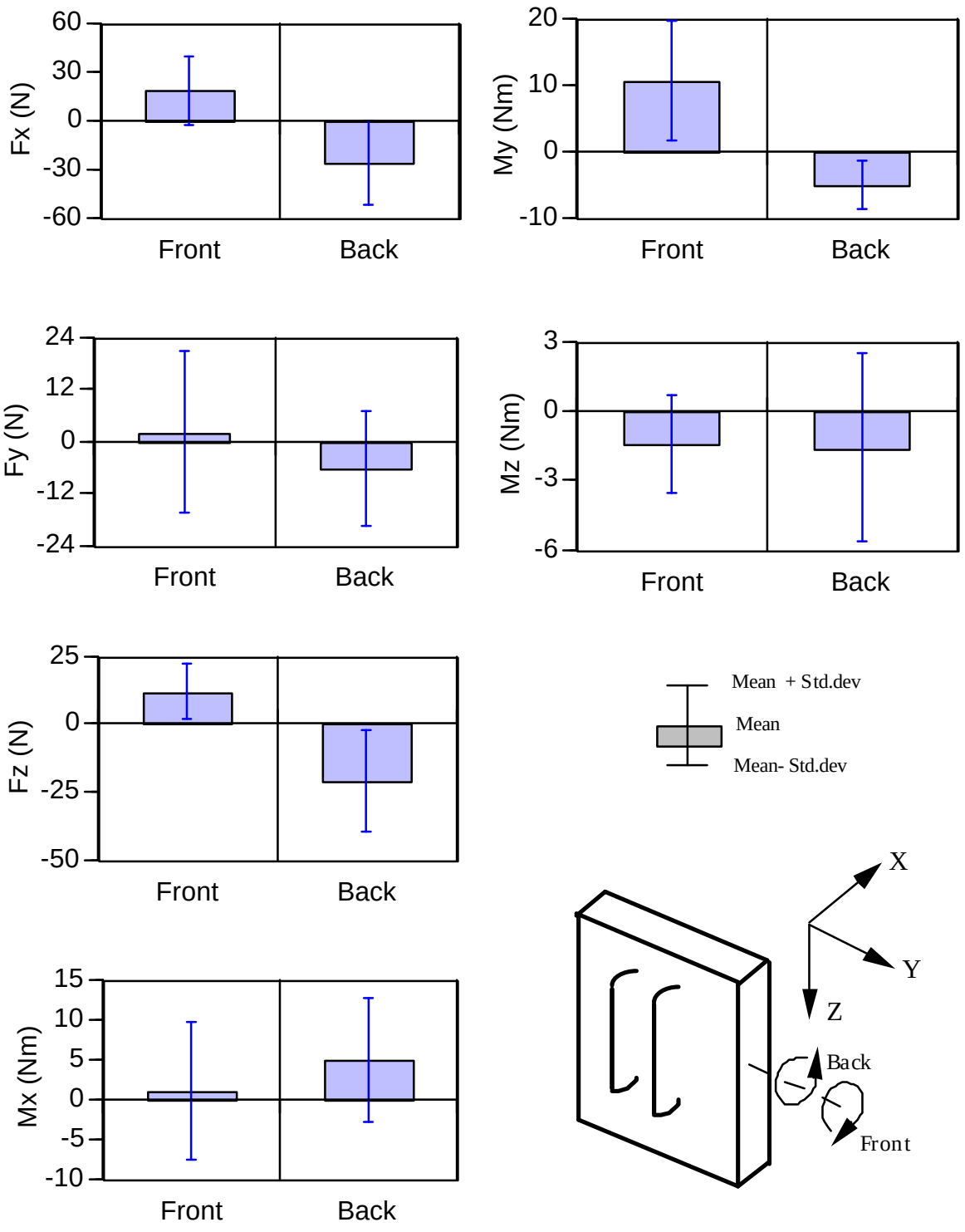

Figure 13. Forces and moments during pitch rotation tasks

The pitching moment (M_y) was greater when pitching forward than when pitching backward. Table 9 provides descriptive statistics on the forces and moments during these tasks.

Table 9: Summary of average and standard deviation of forces and moments during various tasks

Push/Pull Translation

	Push			Pull		
Variable	**Mean**	**Std.Dev**	**Range**	**Mean**	**Std.Dev**	**Range**
F_x	1.78	6.94	-12.03 8.64	2.41	4.28	-4.66 11.02
F_y	-15.25	35.34	-64.80 46.84	-47.85	15.10	-72.41 -29.31
F_z	42.95	18.36	20.01 72.56	-42.50	14.39	-64.63 -23.02
M_x	-3.96	5.72	-10.35 8.71	-3.06	5.52	-12.52 3.84
M_y	0.59	7.46	6.56 -1.69	-5.37	2.06	-8.29 -1.41
M_z	0.66	1.21	-1.77 2.77	1.39	2.83	-2.19 6.78

Side to Side Translation

	Right			Left		
Variable	**Mean**	**Std.Dev**	**Range**	**Mean**	**Std.Dev**	**Range**
F_x	30.99	10.13	15.71 46.57	-33.09	11.13	-50.31 -15.34
F_y	-25.25	16.09	-48.97 -1.88	-28.13	22.39	-60.95 12.22
F_z	-4.62	9.79	-24.48 10.03	-2.48	10.46	-27.57 12.62
M_x	-2.21	1.61	-5.36 0.31	-5.53	7.29	-19.54 3.56
M_y	5.94	3.88	-3.19 10.78	-6.34	4.93	-14.32 -0.77
M_z	3.35	2.38	0.29 7.43	-0.19	5.30	-6.02 9.81

Yaw Rotation

	Right			Left		
Variable	**Mean**	**Std.Dev**	**Range**	**Mean**	**Std.Dev**	**Range**
F_x	16.34	24.23	-15.96 50.07	-33.99	21.68	-74.55 -10.97
F_y	9.11	15.22	30.45 -30.70	56.54	-28.16	21.68 -58.51
F_z	7.23	12.53	-3.35 45.77	-4.45	13.25	-32.13 11.80
M_x	5.53	5.77	-3.52 12.33	-4.64	4.49	-11.45 3.74
M_y	4.23	14.15	-17.48 26.83	-11.69	6.93	-17.04 8.39
M_z	3.63	2.51	-1.44 7.60	1.13	1.83	-1.26 4.85

Table 9: Summary of average and standard deviation of forces and moments during various tasks (Continued)

Roll Rotation

	Right				Left			
Variable	**Mean**	**Std.Dev**	**Range**		**Mean**	**Std.Dev**	**Range**	
F_x	27.80	21.46	-1.95	59.97	-12.82	22.77	-47.48	28.60
F_y	-6.72	14.58	-32.49	22.29	-16.14	14.37	-47.78	6.92
F_z	-6.40	32.09	-70.00	26.09	-23.65	33.39	114.20	17.99
M_x	5.91	2.76	1.39	9.88	4.05	4.68	-0.04	16.57
M_y	-3.49	3.72	-12.08	1.39	-1.59	4.84	-12.16	3.71
M_z	12.42	6.79	-1.66	20.18	-8.92	5.27	-16.63	0.24

Pitch Rotation

	Right				Left			
Variable	**Mean**	**Std.Dev**	**Range**		**Mean**	**Std.Dev**	**Range**	
F_x	2.09	18.41	-18.59	34.91	-6.29	13.32	-27.76	8.47
F_y	11.87	10.26	-0.08	35.13	-20.98	19.03	-43.99	10.57
F_z	18.53	21.21	-25.33	46.73	-26.41	26.25	-77.17	3.98
M_x	10.45	8.98	-6.50	22.16	-5.08	3.72	-11.77	-0.06
M_y	-1.40	2.09	-4.53	2.81	-1.57	4.06	-9.58	4.82
M_z	1.10	8.55	-5.59	27.04	4.89	7.72	-2.48	21.42

4.2 RMS Run Start/Stop Tasks

Statistical analyses of the RMS data set showed that, as a whole, the three force and the three moment components did not change significantly as a function of velocity (Wilk's test: $F(6,1) = 1.42$; $p < 0.5666$). However, these dependent measures were significantly affected by a change in the phase of motion (Wilk's test: $F(12,2) = 46.82$; $p < 0.0202$). While testing for the statistical significance of these two independent variables, the three-way interaction between subject, phase, and velocity (subject*phase*velocity) was used as the error term. In addition to these two independent variables (velocity and phase of translation), the overall influence of subject variation was also tested, and analyses showed that subject variation did not affect the dependent measure set significantly (Wilk's test: $F(18,3) = 5.16$; $p < 0.859$). Graphical representations of these data can be seen in Figures 14 and 15. These figures show the average and standard deviations for all three forces and moments for each task.

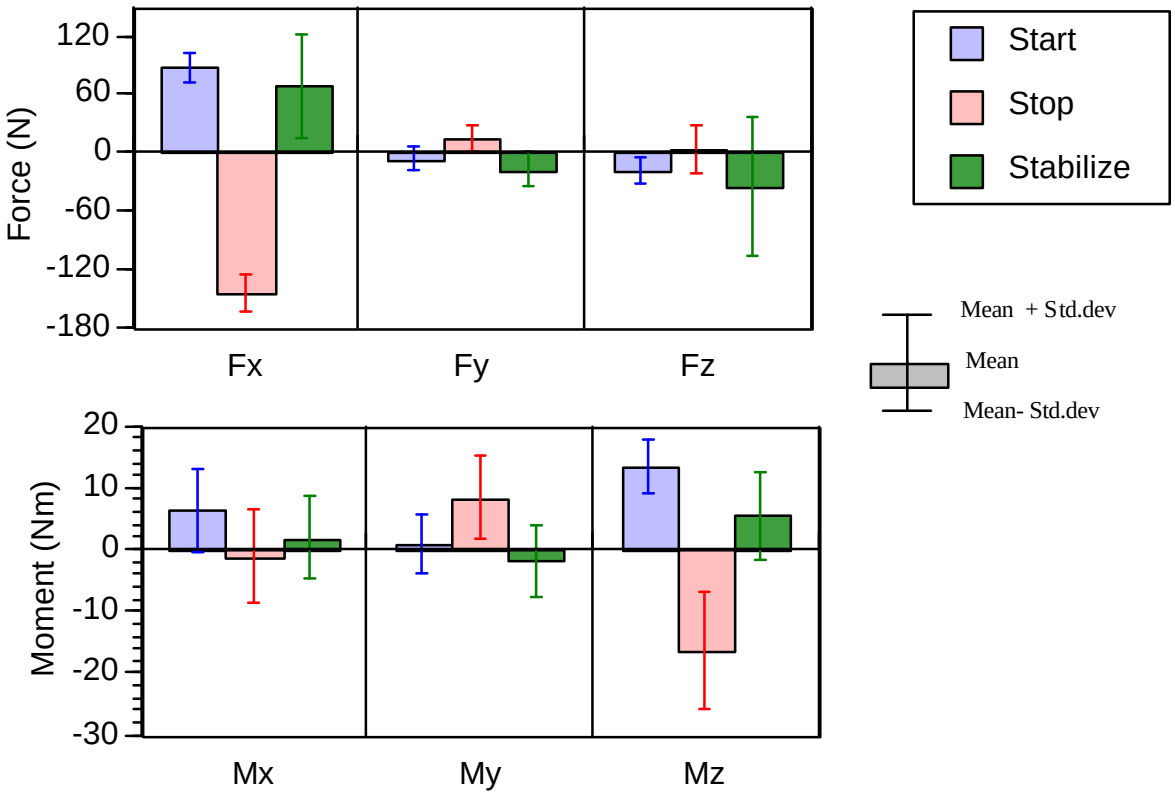

Figure 14. Forces and moments during RMS run start/stop conditions as a function of phases

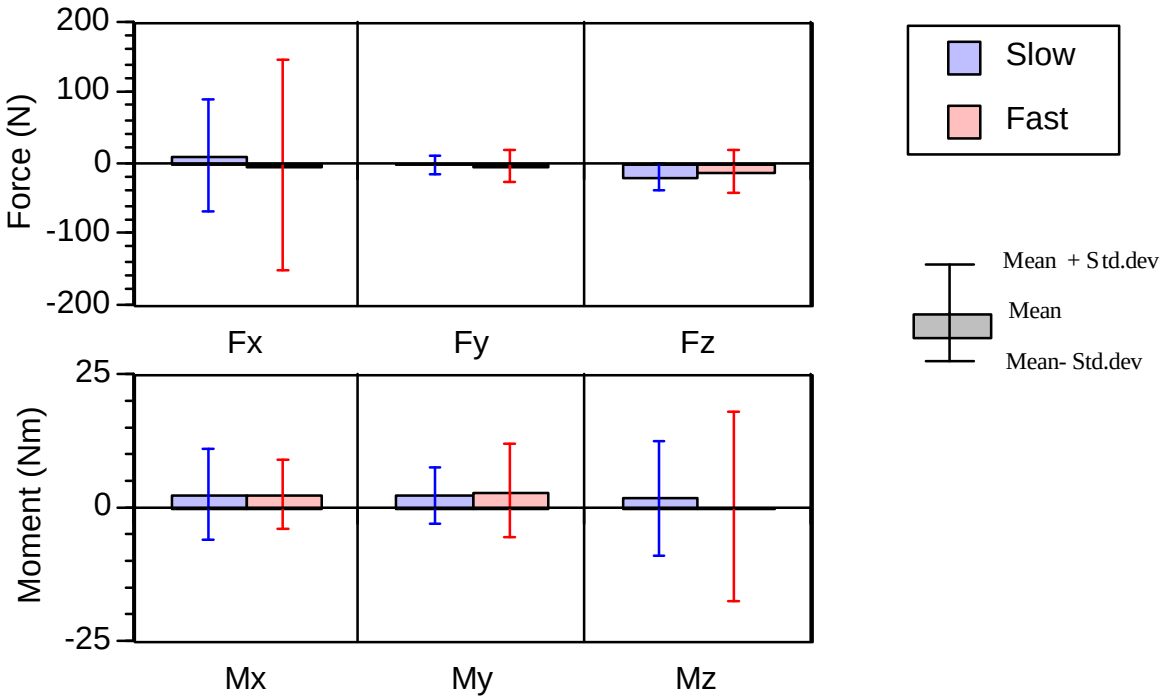

Figure 15. Forces and moments during RMS run start/stop as a function of velocity

Subsequent univariate analyses showed that all the force and moment components were significantly affected by a change in phase ($p < 0.0001$; Table 10). Only F_z was significantly affected by a change in velocity ($p < 0.04$).

Table 10: Analysis of variance results for RMS data set: level of significance

Dependent Variable	Independent Variables		
	Velocity p =	Phase p =	Subject p =
F_x		0.0001	0.046
F_y		0.004	
F_z	0.04	0.0001	0.013
M_x		0.0001	
M_y		0.001	0.001
M_z		0.0012	

Since velocity did not affect a majority of the dependent measures significantly, no data on dependent measures as a function of velocity will be reported here. With a change in phase from starting to stabilizing, the response of F_x was significantly different and the pattern of response was drastically different from the patterns of response for F_y and F_z. Table 11 shows that more force was exerted in the x direction during stopping and starting than during the stabilizing phase (-145 N or 87.2 N vs. 68 N).

F_y significantly changed, not only in magnitude but also in direction (Table 12). The force was greater during stopping than during starting (14.5 N vs. -6.5 N). Slightly higher (and statistically significant) forces were recorded for stabilization than those recorded for stopping (-18.2 N vs. 14.5 N).

F_z also changed significantly as a result of a change in phase (Table 13). F_z was greater during starting than during stopping (-18.6 N vs. 4.0 N). As in the case of F_y, F_z was much greater during the stabilizing phase than during the other two phases (-36.0 N vs. -18.6 or 4.0 N).

Compared to M_y and M_z, M_x was considerably lower, ranging from -1.1 to 6.3 Nm (Table 14). For the moment about the Y axis, which ranged from -1.8 Nm to 8.4 Nm, greater moments were generated during stopping than during the other two phases (Table 15). For M_z, which ranged from -16.4 to 13.4 Nm, greater moments were generated during stopping than during the other two phases (Table 16).

Table 11: Mean F_x as a function of phase

Phase	Mean Value	Grouping[5]
Starting	87.2	A
Stopping	-145.0	C
Stabilizing	67.9	B

Table 12: Mean F_y as a function of phase

Phase	Mean Value	Grouping[5]
Starting	-6.5	B
Stopping	14.5	A
Stabilizing	-18.2	C

Table 13: Mean F_z as a function of phase

Phase	Mean Value	Grouping[5]
Starting	-18.6	B
Stopping	4.0	A
Stabilizing	-36.0	C

[5]Same letter grouping denotes there is no statistical significance within the same grouping.

Table 14: Mean M_x as a function of phase

Phase	Mean Value	Grouping[6]
Starting	6.3	A
Stopping	-1.1	C
Stabilizing	1.9	B

Table 15: Mean M_y as a function of phase

Phase	Mean Value	Grouping[6]
Starting	0.9	B
Stopping	8.4	A
Stabilizing	-1.8	C

Table 16: Mean M_z as a function of phase

Phase	Mean Value	Grouping[6]
Starting	13.4	A
Stopping	-16.4	C
Stabilizing	5.4	B

[6]Same letter grouping denotes there is no statistical significance within the same grouping.

5.0 Discussion

One objective of this study was to simulate and monitor the reaction of an EVA crew member who is maneuvering the ORUs and during an RMS sudden start/stop condition. More specifically, the purpose was to determine whether an EVA crew member who is standing in the PFR at the end of the RMS could safely maneuver the ORU if the RMS suddenly started or stopped. In addition, as mentioned earlier, this study was aimed at providing additional training for the STS-61 astronauts to supplement their WETF training or to offset the negative training possibly derived from the WETF, or both.

To understand and appreciate the effect of this scenario, mass handling characteristics were first studied under a controlled fashion. From the results of this study, several interesting observations were apparent. In general, as would be expected, the mean force components were greater during translation than during rotation tasks and the mean moment components were greater during rotation than during translation tasks. The mean force in the push/pull direction was the highest, with the exception of forces in the up and down directions. The experimental setup was most likely the major factor contributing to such high up and down forces.

Even though the PABF simulated the friction-free aspect of zero-g space, the effect of gravity was still present in the vertical plane. The large force component along the vertical axis was primarily a result of test subjects transferring the load of their suits to the handrails. The suit weighs about 68 kg. Much of this load is located in the back; however, a significant amount is located around the arms and shoulders. To overcome fatigue in their arm muscles and to keep their elbows parallel to the floor, subjects held onto the handrails for support, thus inducing a large force along the vertical axis. In zero g, where the weight of the suit is not an issue, the only vertical force is the force a crew member intends to exert.

When compared to the mean forces involved during translation and rotation activities, the force in the push/pull direction was three times greater during RMS start/stop conditions. However, forces in the vertical and transverse axes were less than those observed during controlled translation and rotation tasks.

The above inferences were based on data that represent overall mean data. At times, the overall peak information provides a different perspective from that seen in the overall mean data. Tables 17 and 18 show the overall peak values for all six force and moment components and indicate the task under which the peak occurred. As can be seen from these tables, the maximum force measured during controlled motions was about 114 N, whereas during RMS conditions the maximum force measured was 296 N. There were no differences

in moment components between controlled motion and RMS conditions. It is apparent that, with the exception of push/pull force, the rest of the force components and all moment components were similar to what might be expected during a slow, controlled translation or rotation task. The most important question that needed to be answered, however, was how severe the push/pull force was during a sudden RMS run start/stop condition. The following discussion is aimed at answering that question.

Table 17: Peak forces and moments during translation and rotation tasks

Force/Moment Component	Condition	Value
F_x	Roll	-114.2 N
F_y	Yaw	-74.6 N
F_z	Push/pull	-72.4 N
M_x	Pitch	27.0 Nm
M_y	Pitch	22.2 Nm
M_z	Yaw	26.8 Nm

Table 18. Peak forces and moments during different phases of RMS run start/stop tasks

Force/Moment Component	Condition	Value
F_x	Stop	-296.0 N
F_y	Stop	54.0 N
F_z	Stabilize	-70.5 N
M_x	Start	32.1 Nm
M_y	Stop	22.9 Nm
M_z	Stop	33.9 Nm

The maximum force observed at the handrails of the COSTAR ORU during RMS run start/stop conditions was 296 N. This force was exerted pri-

marily to arrest the motion of the ORU and to prevent the ORU from moving farther away from the subject. In other words, during a sudden RMS run start/stop condition, 296 N of hand grasp strength was exerted to prevent the ORU handrails slipping away from the subject's hands. In an earlier study (Rajulu and Klute, 1992) conducted in the Anthropometry and Biomechanics Lab on hand grasp breakaway strength, the hand grasp breakaway capability of a man was 1026 N and of a woman was 696 N. Thus, the worst-case load on EVA crew members who are handling an ORU is only 29% of what a male crew member is capable of and only 43% of what a female crew member is capable of. These data indicate that EVA crew members will be able to maintain their grasp on the COSTAR ORU during a sudden RMS start or stop. Judging by these data, it seems that, even during a fast and sudden RMS start/ stop condition, the nature of impact is not as severe as might have been expected. The following discussion further explains that the maximum hand grasp force required in space will be much less than 296 N.

The test setup of the PABF influenced the amount of hand force exerted by subjects. During testing, the subjects stood on an air bearing sled and had two lines of restraint. The first line of restraint was a weight relief from above the subject, and the second was a mid-torso restraint which prevented the subject from falling forward or backward. Without these restraints, test subjects would have risked injury. During the test when the RMS motion was suddenly started or stopped, the two restraints provided a load path that would not be present on orbit. Without these restraints, most of the forces would have been transmitted to the foot restraint and not to the handrails. Therefore, the maximum hand force (296 N) is higher than what would be possible on orbit because of these two load paths. To compensate for the influence of this effect, a biomechanical model was used to predict likely forces present at the handrails during an actual task.

With no relief system to restrain the subjects, the force at the COSTAR handrails would have to be reacted to by a torque about the ankle joint. Otherwise, there would be a pitching motion at the foot restraint (i.e., the subject would fall forward). This pitching motion would be reacted to by an eccentric dorsiflexion of the ankle and aided by the gastrocnemius and soleus muscles. Data on the ability of crew members to perform eccentric dorsiflexion pre- and postflight are available from [detailed supplementary objective] DSO-477 (1992). DSO-477 measured the torque produced during an eccentric dorsiflexion of 17 crew members at an isokinetic velocity of 30 deg/s. The resulting peak torque from all test subjects was 89.7 Nm. Additionally, there were no significant differences between pre- and postflight data. From this it was concluded that the HST crew would experience no appreciable degradation during flight. With a 1.22 m moment arm from the PFR to the handle position, the EVA crew could generate only 74.2 N (89.7/1.22) of force at the COSTAR handrails. This was significantly less than the 296 N generated in the PABF test.

Further consideration of DSO-477 data revealed that the 89.7 Nm torque is the peak torque exerted during torque measurements throughout a crew member's ankle range of motion. A reasonable assumption of the average torque that can be exerted through most of the range of motion is 50% of the peak, or 44.9 Nm. This value will be used in the following analysis.

Since the HST EVA crew members did not have restraints of any kind other than the ones at their feet, safe deceleration of the ORU involved the angle at which the EVA crew would have been pitched over during a sudden RMS stop. This angle is a function of the RMS velocity. At a sufficiently slow velocity, the eccentric dorsiflexion torque capability is equivalent to isometric torque capacity, which in turn is greater than dynamic torque capacity. Hence, if the velocity is sufficiently slow, the eccentric dorsiflexion torque to safely decelerate the ORU is within an EVA crew's capability. Therefore, the question becomes the velocity envelope in which RMS operations can be conducted that will preclude the possibility of the EVA crew being pitched over into an unacceptable position or posture.

During a forward translation of the RMS (positive Z axis; Figure 7), the crew member and the ORU can be modeled as a rigid body with known mass and inertia. The COSTAR mass is 299 kg and its X axis inertia is 156 kg $*$ m^2. Human mass and inertia data can be found in the Man Systems Integration Standards (1992). Calculations with the inertia transfer formula, which yield an inertia rotating about the PFR, result in an X axis inertia of 1535.0 kg $*$ m^2. Using Newtonian physics, the equation relating the pitch over angle to velocity is:

$$\mathbf{\emptyset = \frac{1}{2} \frac{(V_t)^2 (I)}{(R)^2 (T)} \frac{180}{(p)}}$$

or

$$\emptyset = 423.56 (V_t)^2 \text{ if } V_t \text{ is in m/s}$$

$$= 39.30 (V_t)^2 \text{ if } V_t \text{ is in fps}$$

where: $\emptyset$ is the pitchover angle (deg),
V_t is the RMS velocity (m/s),
R is the distance 0.274 m (5 ft) from the PFR to the system center of mass,
T is the average torque 44.85 Nm exerted throughout $\emptyset$, and
I_x is the system inertia 1535 kg m^2 calculated about an axis of rotation centered at the PFR.

The primary objective of this investigation was to provide an answer to the following question: Under a sudden RMS start or stop condition, will an EVA crew member be able to safely decelerate and stabilize the ORU? As stated earlier, the criteria for safely decelerating and stabilizing the ORU should be

based on the range of motion of a crew member's ankle. The pitch of the PFR (plantar flexion of 21 deg; ref. 3, sec. 3.3.4.3), and the 5th percentile male's dorsiflexion range of motion (8 deg; ref. 3, sec. 3.3.2.3.1), yields an extremely conservative range of motion of 29 deg. Therefore, a crew member who has an average torque capability (44.85 Nm) and a minimal ankle range of motion (29 deg) can safely decelerate and stabilize the COSTAR with an RMS velocity equal to or slower than 0.261 m/s. The pitchover angle at nominal RMS velocity 0.152 m/s is 9.8 deg.

6.0 Conclusion

In this study, we were able to accomplish our objective of simulating ORU mass handling characteristics in the PABF. The mockups, which were similar to the actual ORU mass characteristics, allowed crew members to experience the effect of no friction on their performance. Also, in this study we obtained quantitative data to determine the impact of a sudden RMS run start/stop situation on a crew member. From data collected, we concluded that the HST EVA crew would be able to decelerate safely and to stabilize the COSTAR ORU during nominal RMS operations (velocity equal to 0.152 m/s or 0.5 fps). Additionally, RMS velocities up to 0.26 m/s or 0.9 fps could be accommodated under sudden stop conditions without pitching the crew member over beyond an analytically conservative range of motion.

7.0 References

1. Hayes, J. C.; McBrine, J. J.; Roper, M. L.; Harris, B. A.; Siconolfi, S. F.; and Greenisen, M. C. Final Report – DSO 477: The Evaluation of Concentric and Eccentric Skeletal Muscle Contractions Following Space Flight. Johnson Space Center, 1992.

2. Rajulu, S. L.; and Klute, G. K. A Comparison of Hand Grasp Breakaway Strengths and Bare-handed Grip Strengths of the Astronauts, SML III Test Subjects, and the Subjects From the General Population. NASA Technical Paper 3286, 1993.

3. Man Systems Integration Standards (MSIS), NASA-STD-3000, Chapter 3: Anthropometry and Biomechanics, Volume I, Rev. A, October 1989.

Appendix A

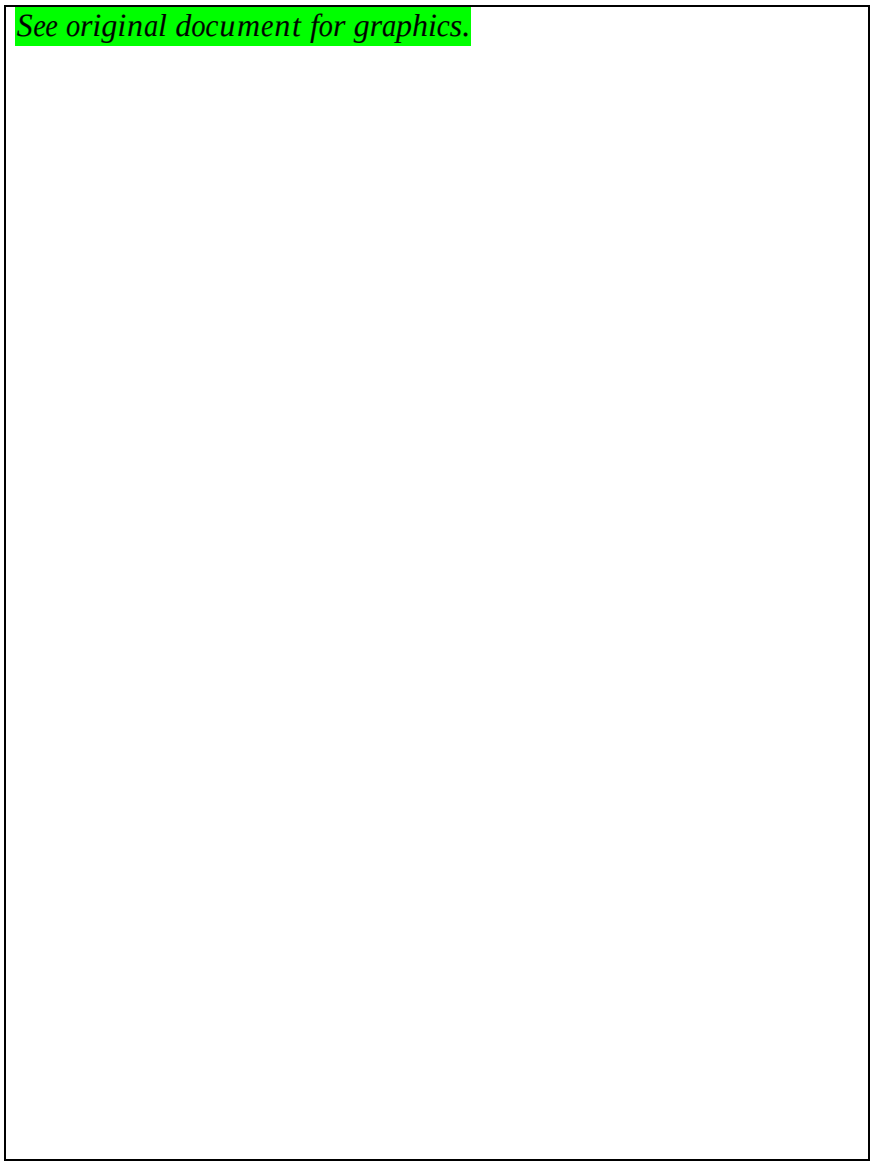

Figure A1. The Hubble Space Telescope (HST)

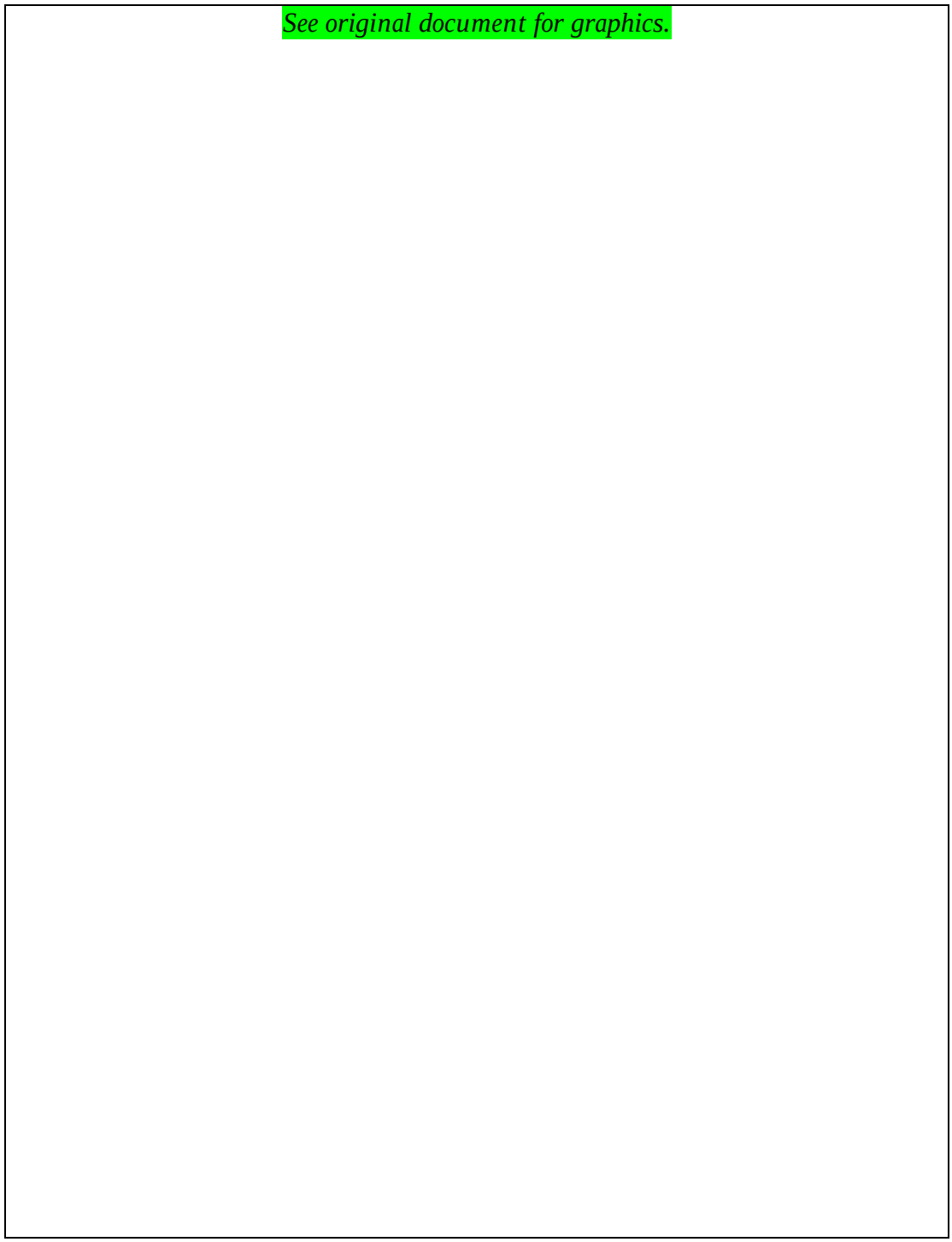

Figure A2. The COSTAR housed in the HST

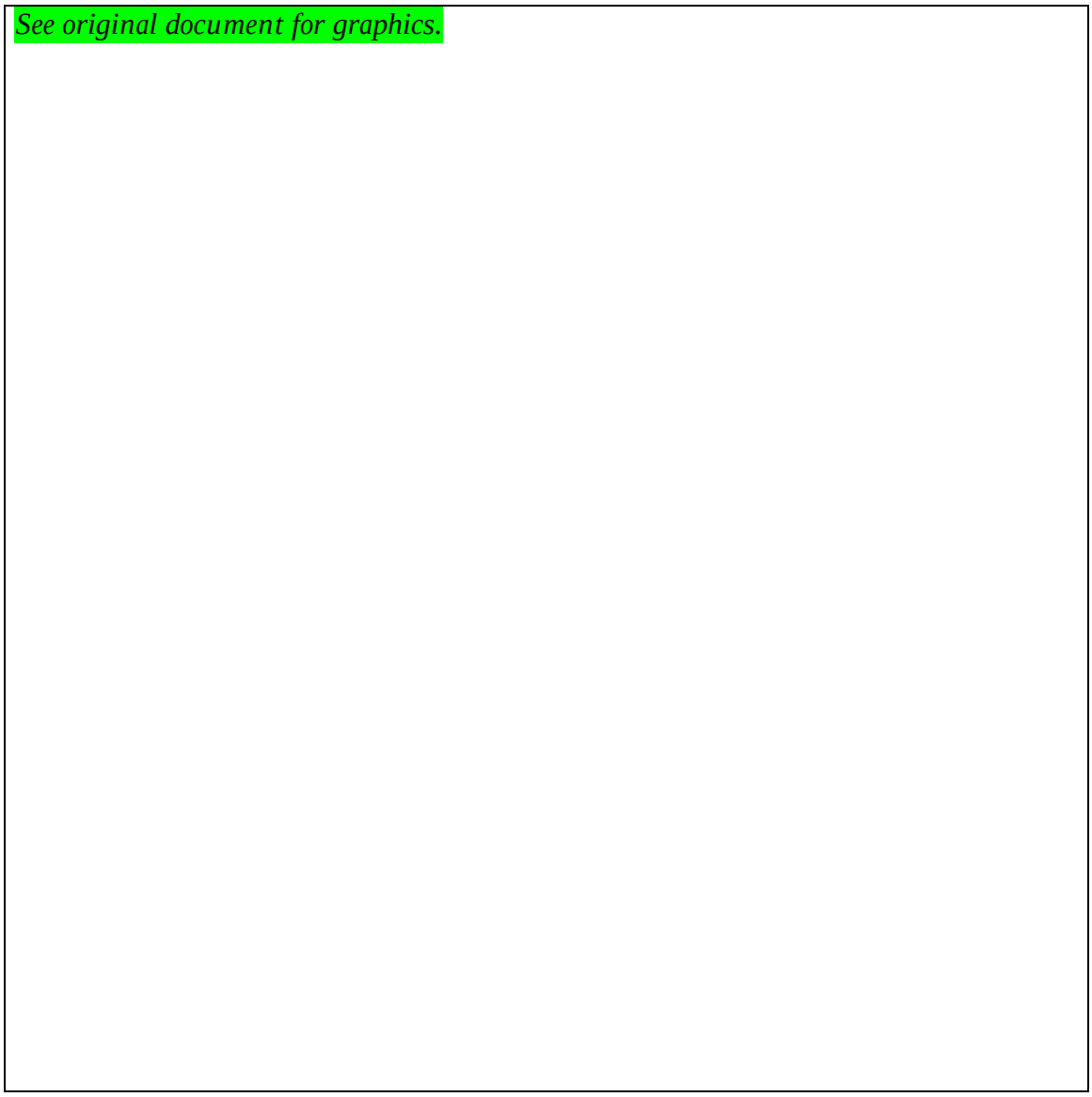

Figure A3. The WF/PC

Figure A4. The solar arrays and HST in orbit

Appendix B

COSTAR Mockup Inertia Report
by
Lauren Fletcher

Purpose:

A mockup of the Corrective Optics Space Telescope Axial Replacement (COSTAR) was designed and built to simulate the known inertia of COSTAR on the Precision Air Bearing Facility (PABF). It is necessary that the inertia of this mockup closely matches that of the actual COSTAR, since the purpose of PABF training is to provide the astronauts a chance to experience what the COSTAR will feel like in microgravity. The goal of this project was to calculate the inertia of the mockup and to ensure the validity of the training of the astronauts for their upcoming mission.

Formulas and Methods of Calculations:

The inertia tensor and the parallel-axis theorem were the main formulas used for the calculation of the inertia's. The inertia tensor was solved for the diagonal elements only (X_{11}, X_{22}, and X_{33}), which correspond to the moments of inertia about the X_1, X_2, and X_3 axes, respectively.

The formula for calculating the inertia tensor is given as follows:

$$I_{ij} = \int_V p(r)[d_{ij}\sum_K X_K^2 - X_i X_j]dV$$

I_{ij} is the element for which the inertia is being calculated. As with all bodies considered as a continuous distribution of matter, I_{ij} is integrated in terms of volume and possesses a mass density $p = p(r)$ with $dV = dX_1 dX_2 dX_3$ as the element of volume at the position defined by the vector **r**. The Kronecker delta symbol, d_{ij}, means that, for a given *i* and *j*, d_{ij} will equal zero if $i \neq j$ and will equal 1 if $i = j$.

The parallel axis theorem is given as follows:

$$I = I_{cm} + Mh^2$$

where I_{cm} is the inertia of the body from its own center of mass, *M* is the mass of the body, and *h* is the distance from the center of mass of the body to the axis of rotation.

Using the inertia tensor, the inertia of each part that made up the mockup was calculated about its own center of mass. The parallel-axis theorem was then applied to change the inertia of the part from its own center of mass to the axis of

rotation of the mockup. After that, all the inertia were added up to give the total inertia along the axis of rotation of the mockup.

Drawing Representation:

A numbering system was used to identify the mockup parts. Each intersection was given a number designation (Figure B3). A part was identified by the numbers at its ends. For example, bar 1,4 is the bottom bar directly below the handrails located on the negative X_2 side.

Worksheet:

The worksheet gives the designation of each part, its inertia, its weight, and its contribution of inertia to the entire mockup in each axis of rotation.

Inertia of Force Plate

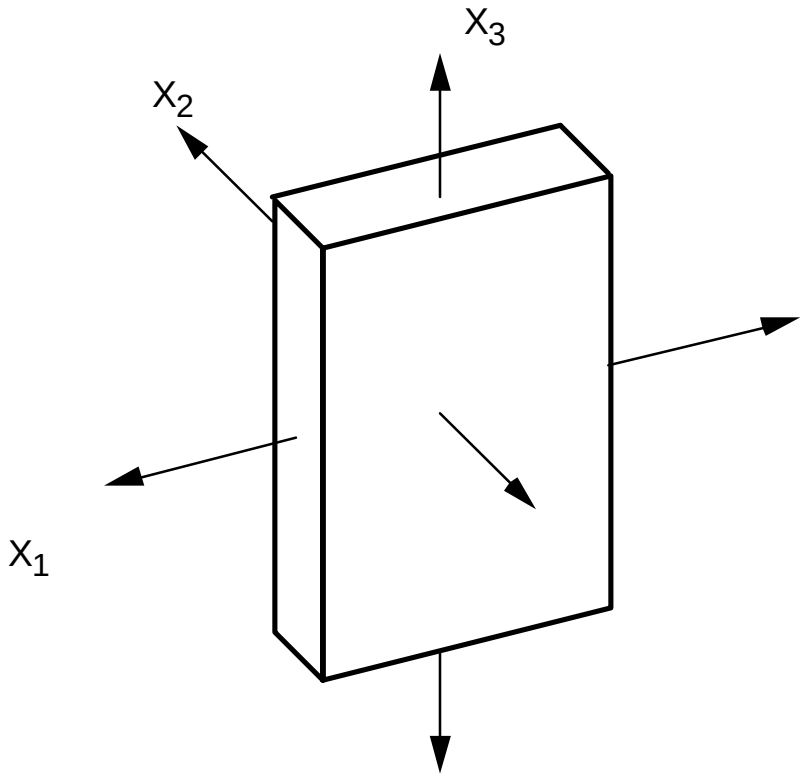

$$F = ma \Rightarrow F = w; a = g$$

$$w = mg$$

$$m = \frac{w}{g} \Rightarrow \begin{matrix} w = 78lbs \\ g = 32.2\frac{ft}{s^2} \end{matrix}$$

$$m = \frac{78lb}{32.2\frac{ft}{s^2}} = 2.422\frac{lbs^2}{ft}$$

$$m = 2.422slug$$

$$p = \frac{m}{v} \Rightarrow v = 0.4016\,ft^3$$

$$p = \frac{2.422slug}{0.4016\,ft^3} = 6.2\frac{slug}{ft^3}$$

limits: in feet

$$x_1 : -0.656 to 0.656$$

$$x_2 : -0.078 to 0.078$$

$$x_3 : -0.979 to 0.979$$

Inertia Calculations Continued

$$I_{11} = r(r)\int_v [x_2^2 + x_3^2]dv$$
$$I_{11} = r(r)\int_{-0.979}^{0.979}\int_{-0.078}^{0.078}\int_{-0.656}^{0.656}[x_2^2 + x_3^2]dx_1 dx_2 dx_3$$

$$I_{11} = r(r)\int_{-0.979}^{0.979}\int_{-0.078}^{0.078}[x_1 x_2^2 + x_1 x_3^2]_{-0.656}^{0.656} dx_2 dx_3$$
$$I_{11} = r(r)\int_{-0.979}^{0.979}\int_{-0.078}^{0.078}[1.312 x_2^2 + 1.312 x_3^2]dx_2 dx_3$$
$$I_{11} = r(r)\int_{-0.979}^{0.979}[.4373 x_2^3 + 1.312 x_2 x_3^2]_{-0.078}^{0.078} dx_3$$

$$I_{11} = r(r)\int_{-0.979}^{0.979}[0.000415043 + 0.204672 x_3^2]dx_3$$

$$I_{11} = r(r)[0.000415043 x_3 + 0.068224 x_3^3]_{-0.979}^{0.979}$$
$$I_{11} = r(r)[0.12842\ ft^5]$$

$$I_{11} = \left(\frac{6.2 slug}{ft^3}\right)\left(\frac{0.12842\ ft^5}{1}\right) = 0.7962 slug ft^2$$

$$I_{22} = p(r)\int_v [x_1^2 + x_3^2]dv$$
$$I_{22} = \int\int\int [x_1^2 + x_3^2]dx_1 dx_2 dx_3$$
$$I_{22} = p(r)\int\int [\frac{1}{3} x_1^3 + x_1 x_3^2]_{-0.656}^{0.656} dx_2 dx_3$$
$$I_{22} = p(r)\int\int [0.1882 + 1.312 x_3^2]dx_2 dx_3$$
$$I_{22} = p(r)\int [0.1882 x_2 + 1.312 x_2 x_3^2]_{-0.078}^{0.078} dx_3$$
$$I_{22} = p(r)\int [0.02936 + 0.20467 x_3^2]dx_3$$
$$I_{22} = p(r)\int [0.02936 x_3 + 0.068224 x_3^3]_{-0.979}^{0.979}$$
$$I_{22} = p(r)[0.18552\ ft^5]$$
$$I_{22} = \left(\frac{6.2 slug}{ft^3}\right)\left(\frac{018552\ ft^5}{1}\right) = 1.1502 slug ft^2$$

Inertia Calculations Continued

$$I_{33} = p(r)\int_v [x_1^2 + x_2^2]dv$$

$$I_{33} = p(r)\int\int\int [x_1^2 + x_2^2]dx_1 dx_2 dx_3$$

$$I_{33} = p(r)\int\int [\frac{1}{3}x_1^3 + x_1 x_2^2]_{-0.656}^{0.656} dx_2 dx_3$$

$$I_{33} = p(r)\int\int [0.1882 + 1.312x_2^2]dx_2 dx_3$$

$$I_{33} = p(r)\int [0.1882x_2 + 0.4373x_2^3]_{-0.078}^{0.078} dx_3$$

$$I_{33} = p(r)\int [0.0150946]dx_3$$

$$I_{33} = p(r)[0.0150946x_3]_{-0.979}^{0.979}$$

$$I_{33} = p(r)[0.029555\,ft^5]$$

$$I_{33} = \left(\frac{6.2slug}{ft^3}\right)\left(\frac{0.029555\,ft^5}{1}\right) = 018325slugft^2$$

Drawings of COSTAR Trainer

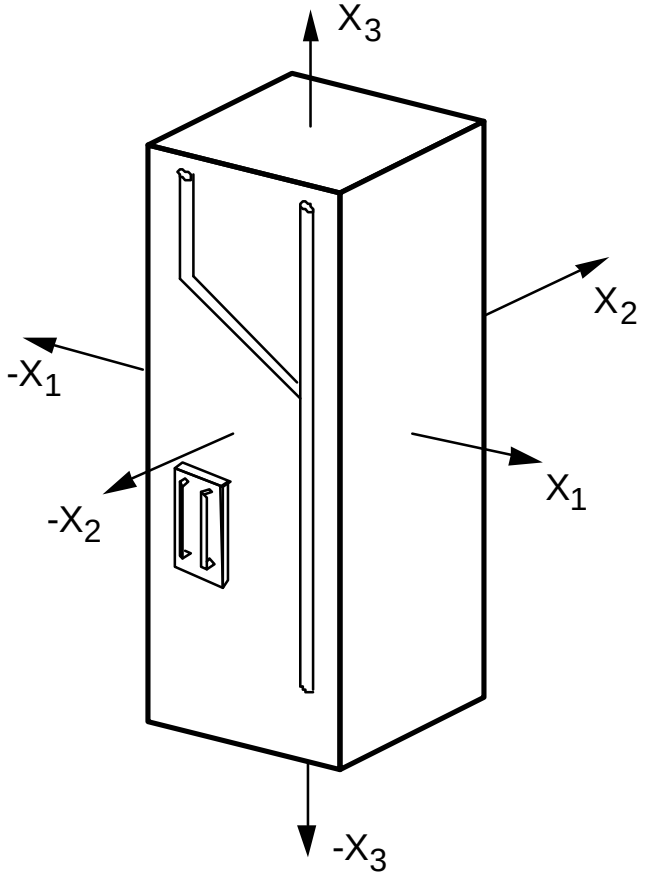

Figure B1. Orientation of axis

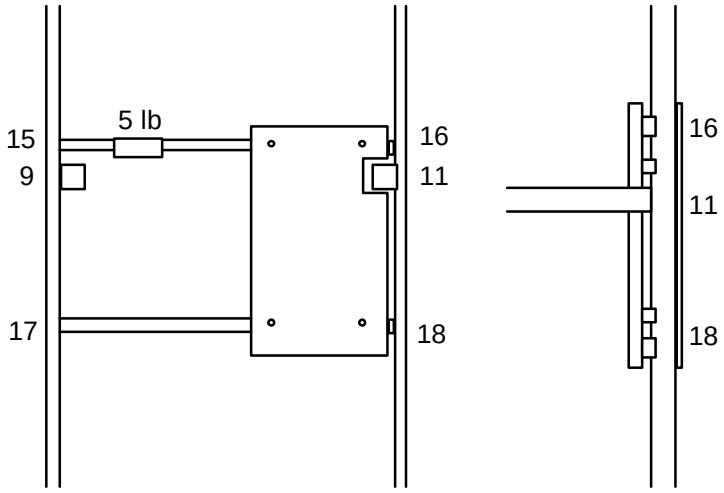

Figure B2. Force plate assembly

Drawings of COSTAR Trainer Continued

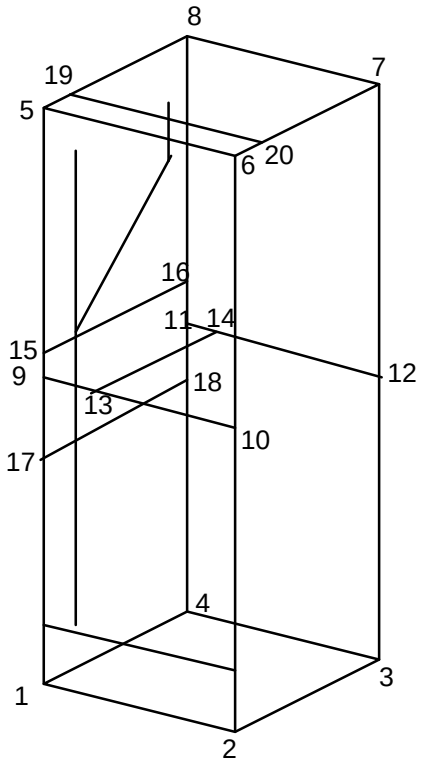

Figure B3. Part numbering system

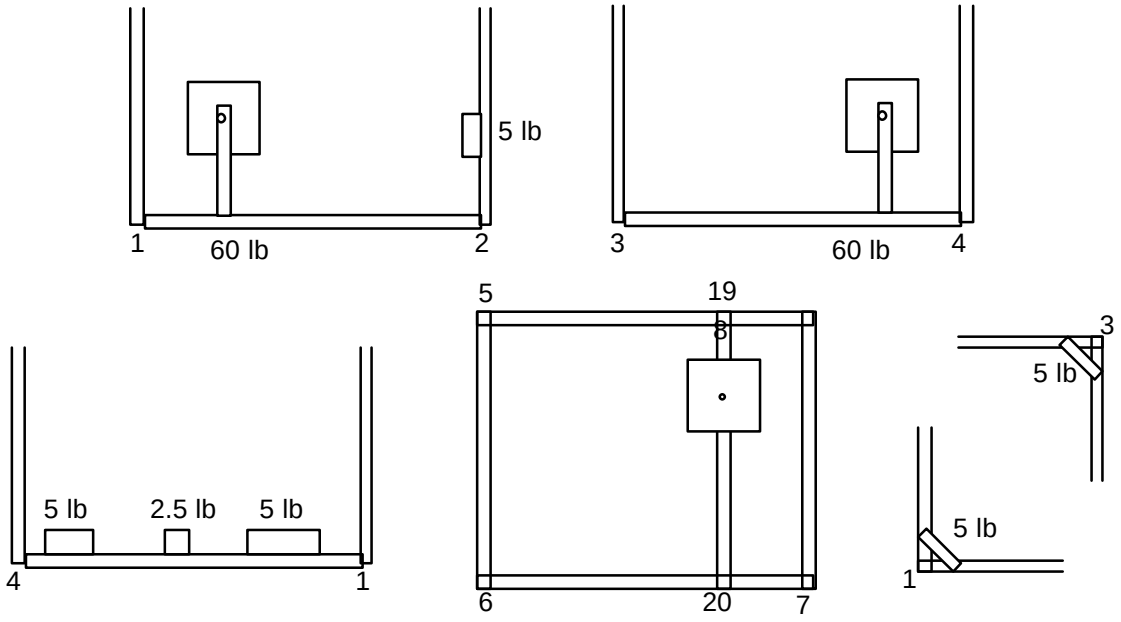

Figure B4. Location and orientation of weights

Results and Conclusions:

With 98% of the weight accounted for, the results yield 113.84, 119.69, and 28.56 slug ft^2 in the X_{11}, X_{22}, and X_{33} axes, respectively. The published values for COSTAR are 115.10, 115.93, and 26.82, respectively. This gives a percent error of 1.09%, 3.24%, and 6.49%, respectively. These results lead to the conclusion that the trainer is well within an expected range of accuracy; however, several sources of error in the calculations should be considered.

All parts were considered to be of uniform density to make the inertia calculations more manageable. As all parts in general are of fairly uniform density and mass distribution, this problem should not throw off the calculations to a noticeable degree.

Another source of error would be the missing weight. As less than 2% of the weight is missing, assuming no extra weight this again should not throw off the calculations. Most of this weight is going to be in the connecting parts, so it is fairly evenly distributed around the trainer.

The final source of error that should be mentioned is that of the sled. The sled comprises about 157 lb of the trainer, which is roughly 24% of the overall weight. It is supposed to be balanced so that the inertia's will be negligible, but that is a difficult thing to do. Primarily, the sled has an effect on the X_{33} axis only because it is rigid and will not rotate around the X_{11} or X_{22} axis. To correct for this, or at least to take it into account, the weight and inertia of the sled should be checked prior to each mockup built using the sled as its base.

REPORT DOCUMENTATION PAGE

Form Approved
OMB No. 0704-0188

1. AGENCY USE ONLY *(Leave Blank)*	2. REPORT DATE	3. REPORT TYPE AND DATES COVERED
	August 1994	NASA Technical Paper

4. TITLE AND SUBTITLE
Evaluation of COSTAR Mass Handling Characteristics in an Environment – A Simulation of the Hubble Space Telescope Service Mission

5. FUNDING NUMBERS

6. AUTHOR(S)
Sudhakar L. Rajulu,* Glenn K. Klute, and Lauren Fletcher

7. PERFORMING ORGANIZATION NAME(S) AND ADDRESS(ES)
Lyndon B. Johnson Space Center
Houston, Texas 77058

8. PERFORMING ORGANIZATION REPORT NUMBERS

9. SPONSORING/MONITORING AGENCY NAME(S) AND ADDRESS(ES)
National Aeronautics and Space Administration
Washington, DC 20546-0001

10. SPONSORING/MONITORING AGENCY REPORT NUMBER
TP-1994-3489

11. SUPPLEMENTARY NOTES
* Lockheed Engineering and Sciences Company, Houston, Texas

12a. DISTRIBUTION/AVAILABILITY STATEMENT
Available from the NASA Center for AeroSpace Information (CASI)
7121 Standard
Hanover, MD 21076-1320

12b. DISTRIBUTION CODE

13. ABSTRACT *(Maximum 200 words)*
The STS-61 mission was for servicing the Hubble Space Telescope (HST), which had been providing valuable information; but modifications were necessary to correct the degraded performance of several components. In addition to servicing orbital replacement units (ORUs), STS-61 crew members replaced the HST solar arrays and performed other maintenance. Without a correction to the optical flaw, usefulness of the HST in the visible light spectrum would have been less than optimal. Also, although NASA had considerable experience in on-orbit extravehicular activities (EVAs), it had never performed such a quantity of complex EVAs as was scheduled for this mission (5 days of EVA and high demands on the crew members and the ground team); it was to be an indication of NASA preparedness to build and maintain a space station. Quality training, therefore, had to be provided so that there were no significant surprises during the tasks of this mission. The purpose of this study was to validate the training techniques for STS-61 crew members in a simulated zero-g environment and to simulate and monitor the reaction of test subjects who were maneuvering the ORU. It was hoped that this study would provide information concerning whether the crew, while moving ORUs, could react to, and counteract comfortably, those forces imparted by the simple motions of mass and inertia. Four subjects participated in our study; tests were conducted on the PABF; mockups were built to simulate the mass characteristics of the COSTAR . Video cameras obtained video data for motion analysis. The main objective of this study was to determine the forces and moments applied and encountered by test subjects during the RMS run start/stop condition.

14. SUBJECT TERMS	15. NUMBER OF PAGES	16. PRICE CODE
Hubble Space Telescope, orbital replacement units, extravehicular activity, spacewalks, International Space Station, zero-g environment, PABF, COSTAR, motion analysis	66	

17. SECURITY CLASSIFICATION OF REPORT	18. SECURITY CLASSIFICATION OF THIS PAGE	19. SECURITY CLASSIFICATION OF ABSTRACT	20. LIMITATION OF ABSTRACT
Unclassified	Unclassified	Unclassified	Unlimited